Synthesis and in Vitro Evaluation of 5-[^{18}F]Fluoroalkyl Pyrimidine Nucleosides for Molecular Imaging of Herpes Simplex Virus Type 1 Thymidine Kinase Reporter Gene Expression

Ann-Marie Chacko,[†] Wenchao Qu,[‡] and Hank F. Kung*[,†,‡]

Departments of Pharmacology and Radiology, University of Pennsylvania, Philadelphia, Pennsylvania 19104

Received April 30, 2008

Two novel series of 5-fluoroalkyl-2′-deoxyuridines (FPrDU, FBuDU, FPeDU) and 2′-fluoro-2′-deoxy-5-fluoroalkylarabinouridines (FFPrAU, FFBuAU, FFPeAU) that have three, four, or five methylene units (propyl, butyl, or pentyl) at C-5 were prepared and tested as reporter probes for imaging herpes simplex virus type 1 thymidine kinase (HSV1-*tk*) gene expression. The Negishi coupling methodology was employed in efficiently synthesizing the radiolabeling precursors. All six 5-[^{18}F]fluoroalkyl pyrimidines were readily prepared from 3-*N*-benzoyl-3′,5′-di-*O*-benzoyl-protected 5-*O*-mesylate precursors in 17−35% radiochemical yield (decay-corrected). In vitro studies highlighted that all six [^{18}F]-labeled nucleosides selectively accumulated in cells expressing the HSV1-TK protein and there was negligible uptake in control cells. [^{18}F]FPrDU, [^{18}F]FBuDU, [^{18}F]FPeDU, and [^{18}F]FFBuAU had the best uptake profiles. Despite their selective accumulation in HSV1-*tk*-expressing cells, all 5-fluoroalkyl pyrimidine nucleosides had low-to-negligible cytotoxic activity (CC_{50} > 1000−1209 μM). Ultimately, the results demonstrated that 5-[^{18}F]fluoropropyl, [^{18}F]fluorobutyl, and [^{18}F]fluoropentyl pyrimidine nucleosides have the potential to be in vivo HSV1-TK PET reporter probes over a dynamic range of reporter gene expression levels.

Introduction

The herpes simplex virus type 1 thymidine kinase (HSV1[a]-*tk*) gene is currently the most actively investigated reporter gene for the noninvasive molecular imaging of gene expression and regulation by modalities such as positron emission tomography (PET).[1] The HSV1-*tk* gene encodes a cytosolic thymidine kinase enzyme HSV1-TK that phosphorylates the pyrimidine nucleoside thymidine (TdR) independently of the ubiquitous cell-cycle-regulated cellular thymidine kinase 1, TK1. The high degree of flexibility of the HSV1-TK active site allows it to phosphorylate not only TdR but also a wide variety of pyrimidine and purine nucleoside derivatives.[2,3] The more restricted substrate specificity of mammalian TK1 (cytosolic)[4] and TK2 (mitochondrial)[5] limits the binding and phosphorylation of non-TdR nucleosides. Both antiviral therapy and suicide gene therapy have taken advantage of the promiscuity of HSV1-TK when it is selectively expressed in herpes-virus-infected cells or cells that are tranduced/transfected with the HSV1-*tk* gene. Prodrugs such as the acyclic purine derivative ganciclovir (GCV) can be activated by phosphorylation only in cells that express the HSV1-TK protein. Following the initial conversion to the monophosphate by HSV1-TK, cellular kinases further phosphorylate the GCV monophosphate to the di- and triphosphate metabolites. The triphosphate form of the nucleoside analog can inhibit DNA polymerase, which results in the chain termination and inhibition of DNA synthesis and cell replication. This and other interactions with key cellular DNA machinery lead to cytotoxicity and cell death.[6,7] Cells that do not express HSV1-TK remain unaffected by the prodrug treatment.

HSV1-*tk* gene expression is a requirement for prodrug activation via its gene product HSV1-TK; analogously, the accumulation of the imaging reporter probe is dependent on the expression of HSV1-*tk* as a reporter gene. To date, a variety of different HSV1-TK PET reporter probes have been reported, and their structures are derived from successful antiviral agents for HSV infection. These include the pyrimidine nucleoside analog of 5-iodo-2′-deoxyuridine[8] (IDU), 2′-fluoro-2′-deoxy-5-[^{124}I]iodo-1-β-D-arabinofuranosyluracil ([^{124}I]FIAU),[9] and the purine analog of GCV 9-(4-[^{18}F]fluoro-3-hydroxymethyl)butyl)guanine ([^{18}F]FHBG).[10,11] Each reporter probe has a unique set of advantages and disadvantages regarding, for example, its routine radiosynthesis, its degree of cellular accumulation (sensitivity), its selective phosphorylation by HSV1-TK versus that by mammalian TKs, its rate of cellular uptake, and its metabolic stability. Recent studies have highlighted 2′-[^{18}F]fluoro-2′-deoxy-5-ethyl-1-β-D-arabinofuranosyluracil ([^{18}F]FEAU)[12−15] and 2′-fluoro-2′-deoxy-5-(2-[^{18}F]fluoroethyl)-1-β-D-arabinofuranosyluracil ([^{18}F]FFEAU)[12,16] as promising imaging agents for the assessment of HSV1-*tk* gene expression. Both [^{18}F]FEAU and [^{18}F]FFEAU, with their two-carbon substituents at C-5, have been shown to accumulate rapidly in HSV1-*tk*-expressing cells in vitro and in vivo with minimal uptake in nontransduced cells. The accumulation and sensitivity characteristics of [^{18}F]FEAU and [^{18}F]FFEAU are similar to those previously reported for FIAU, but [^{18}F]FEAU and [^{18}F]FFEAU have greater selectivity than FIAU because of the lower uptake and retention in nontransduced cells and tissues.[22]

* To whom correspondence should be addressed. Address: Department of Radiology, University of Pennsylvania, 3700 Market Street, Room 305, Philadelphia, PA 19104. Tel: (215) 662-3096. Fax: (215) 349-5035. E-mail: kunghf@sunmac.spect.upenn.edu.

[†] Department of Pharmacology.

[‡] Department of Radiology.

[a] Abbreviations: HSV1, herpes simplex virus type 1; *tk*, thymidine kinase gene; PET, positron emission tomography; TK, thymidine kinase protein; TdR, thymidine; GCV, ganciclovir; IDU, 5-iodo-2′-deoxyuridine; [^{124}I]-FIAU, 2′-fluoro-2′-deoxy-5-[^{124}I]iodo-1-β-D-arabinofuranosyluracil; [^{18}F]-FHBG, 9-(4-[^{18}F]fluoro-3-hydroxymethyl)butyl)guanine; [^{18}F]FEAU, 2′-fluoro-2′-deoxy-5-ethyl-1-β-D-arabinofuranosyluracil; [^{18}F]FFEAU, 2′-fluoro-2′-deoxy-5-(2-fluoroethyl)-1-β-D-arabinofuranosyluracil; BVDU, 5-bromovinyl-2′-deoxyuridine; [^{18}F]FPrDU, 5-(3-fluoropropyl)-2′-deoxyuridine; [^{18}F]FBuDU, 5-(4-fluorobutyl)-2′-deoxyuridine; [^{18}F]FPeDU, 5-(5-fluoropentyl)-2′-deoxyuridine; [^{18}F]FFPrAU, 2′-fluoro-2′-deoxy-5-(3-fluoropropyl)-1-β-D-arabinofuranosyluracil; [^{18}F]FFBuAU, 2′-fluoro-2′-deoxy-5-(4-fluorobutyl)-1-β-D-arabinofuranosyluracil; [^{18}F]FFPeAU, 2′-fluoro-2′-deoxy-5-(5-fluoropentyl)-1-β-D-arabinofuranosyluracil.

10.1021/jm800501d CCC: $40.75
Published on Web 08/23/2008

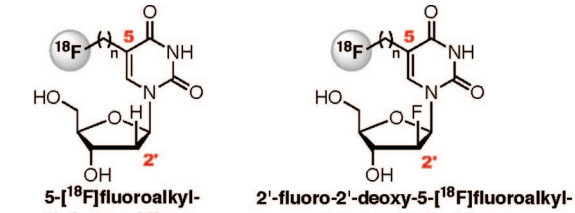

Figure 1. Chemical structures of 5-[^{18}F]fluoroalkyl pyrimidine nucleosides **[^{18}F]1a−f**.

Crystal structure data of HSV1-TK complexed with TdR and 5-bromovinyl-2′-deoxyuridine (BVDU) emphasize a considerable volume of the hydrophobic P1 subpocket remaining around the C-5 substituent for ligand binding to the enzyme.[17−19] We rationalize that pyrimidine nucleosides with nonpolar alkane chains with more than two carbons at C-5 will more closely fit the HSV1-TK enzyme pocket and will improve the substrate binding affinity and the subsequent phosphorylation; their binding to mammalian TKs would be negligible because these kinases do not possess the P1 subpocket.

In this article, we describe our efforts to elucidate the structural requirements for enhanced HSV1-TK reporter probe efficacy by the use of in vitro screening assays. We have synthesized and evaluated two novel series of 5-fluoroalkyl pyrimidine nucleosides that have three (propyl), four (butyl), or five (pentyl) carbon units at C-5 and a C-2′ hydrogen or fluorine atom in the arabino, or "up", position, as depicted in Figure 1. We have designed the 5-[^{18}F]fluoroalkyl-2′-deoxyuridines [^{18}F]FPrDU, [^{18}F]FBuDU, and [^{18}F]FPeDU (**[^{18}F]1a−c**, respectively) and the 2′-fluoro-2′-deoxy-5-[^{18}F]fluoroalkylarabinouridines [^{18}F]FFPrAU, [^{18}F]FFBuAU, and [^{18}F]FFPeAU (**[^{18}F]1d−f**, respectively) for three reasons: (1) to prepare **[^{18}F]1a−f** rapidly and efficiently by convenient radiochemistry in the last stages of radiopharmaceutical synthesis to increase radiochemical yields and to shorten preparation times, (2) to improve the affinity and selectivity of HSV1-TK over mammalian TKs, and (3) to assess the resistance to defluorination and glycosidic bond cleavage in vivo for the 2′-hydrogen versus the 2′-fluorine pyrimidine nucleosides.

Results and Discussion

Chemistry. We have recently developed a methodology to access conveniently two series of 5-fluoroalkylated pyrimidine nucleosides **3a−c** and **3d−f** from core nucleoside precursors that are locked in the β-configuration about C-1′.[20] Negishi cross-coupling reactions of the key tribenzoyl-protected intermediates 3-*N*-benzoyl-3′,5′-di-*O*-benzoyl-5-iodo-2′-deoxyuridine (**2a**) and 3-*N*-benzoyl-3′,5′-di-*O*-benzoyl-2′-fluoro-2′-deoxy-5-iodo-1-β-D-arabinofuranosyluracil (**2b**) with fluoroalkylzinc reagents in the presence of bis(tri-*tert*-butylphosphine)palladium (Pd(P(*t*-Bu)$_3$)$_2$) afforded the two series of nucleosides **3a−f** in one step (Scheme 1). The subsequent treatment of **3a−f** with 0.5 N NaOMe in MeOH selectively cleaved the benzoate groups without affecting the 5-fluoroalkyl moiety to produce the fully deprotected 2′-deoxyuridine analogs 5-(3-fluoropropyl)-2′-deoxyuridine (FPrDU, **1a**), 5-(4-fluorobutyl)-2′-deoxyuridine (FBuDU, **1b**), and 5-(5-fluoropentyl)-2′-deoxyuridine (FPeDU, **1c**) as well as the 2′-fluoro-2′-deoxyarabinouridine analogs 2′-fluoro-2′-deoxy-5-(3-fluoropropyl)-1-β-D-arabinofuranosyluracil (FFPrAU, **1d**), 2′-fluoro-2′-deoxy-5-(4-fluorobutyl)-1-β-D-arabinofuranosyluracil (FFBuAU, **1e**), and 2′-fluoro-2′-deoxy-5-(5-fluoropentyl)-1-β-D-arabinofuranosyluracil (FFPeAU, **1f**) in 85% to quantitative yield.

Scheme 1. Synthesis of 5-Fluoroalkyl Pyrimidine Nucleosides **1a−f**[a]

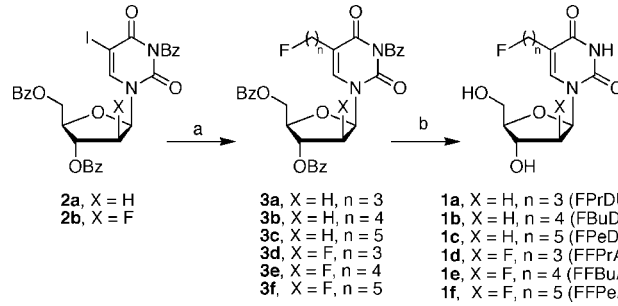

[a] Reagents and conditions: (a) IZn(CH$_2$)$_3$F, BrZn(CH$_2$)$_4$F, or BrZn(CH$_2$)$_5$F; Pd(P(*t*-Bu)$_3$)$_2$; DMA; rt and (b) 0.5 N NaOMe, MeOH, 80 °C.

As depicted in Scheme 2, the 5-silyloxy pyrimidine nucleosides, via the *O*-TBS moiety, offered an easily accessible handle to which we introduced an *O*-mesylate group for subsequent ^{18}F-radiolabeling to achieve the desired HSV1-TK molecular imaging probes **[^{18}F]1a−f**. In our previous work, the Negishi coupling reaction of **2a** with (3-*tert*-butyldimethylsiloxypropyl)-zinc **5a** successfully afforded the *O*-TBS-protected nucleoside **6a** in 45% yield.[20] It was therefore of interest to investigate whether we could extend our optimized coupling methodology to synthesize the two series of *O*-TBS-protected nucleosides **6a−f** for later derivatization.

The bromoalkyl alcohols, which have the alcohol functionality protected as a TBS ether (**4a−c**), were used to prepare the respective alkylzinc bromide reagents **5a−c** by heating at 85 °C with Zn powder and catalytic amounts of I$_2$ in *N,N*-dimethylacetamide (DMA) for 1 h.[20,21] The Negishi coupling reaction of **2a** and **2b** with zinc reagents **5a−c** and catalytic Pd(P(*t*-Bu)$_3$)$_2$ in DMA at room temperature afforded the silylated coupling products **6a−f** in 29−45% yield. The desilylation of the TBS protecting groups of **6a−f** under mild conditions using 1% HCl/EtOH for 2 h at room temperature produced the hydroxylated nucleosides **7a−f** in very high yields. The nucleosides **7a−f**, which have a free hydroxyl moiety, were next converted to 5-*O*-mesylates **8a−f** via a reaction with methanesulfonyl chloride and Et$_3$N in DCM in very high yields (81−99% yield). Interestingly, these mesylates could not afford the cold 5-fluoroalkyl pyrimidines **3a−f** by refluxing **8a−f** in anhydrous TBAF/THF.[22]

This 3-step synthetic approach to the 5-*O*-mesylate radiofluorination precursors that was developed in our research is considerably shorter than reports on the 11-step synthesis of labeling precursors for [^{18}F]FEDU[23] and the more recent 5-step approach to labeling precursors for [^{18}F]FFEAU.[16] Both of these approaches involve the low-yielding glycosylation of a sugar derivative with appropriately protected 5-(2-hydroxyethyl)uracil derivatives followed by a variety of protection and deprotection steps to afford tosylate or tresylate labeling precursors.[16,23]

The [^{18}F]-labeled nucleosides **[^{18}F]1a−f** were prepared in two rapid steps from a one-pot reaction from the tribenzoyl-protected *O*-mesylate nucleosides **8a−f**, as shown in Scheme 3. Briefly, **8a−f** were reacted with [^{18}F]fluoride in the presence of Kryptofix 222 (K[2,2,2]) and potassium carbonate in DMF at 135 °C for 5 min. Radio-HPLC analysis of this crude reaction mixture highlighted multiple [^{18}F]-labeled products including that of the desired [^{18}F]-labeled tribenzoyl-protected nucleosides

Scheme 2. Synthesis of 5-*O*-Mesylate Precursors **8a**−**f**[a]

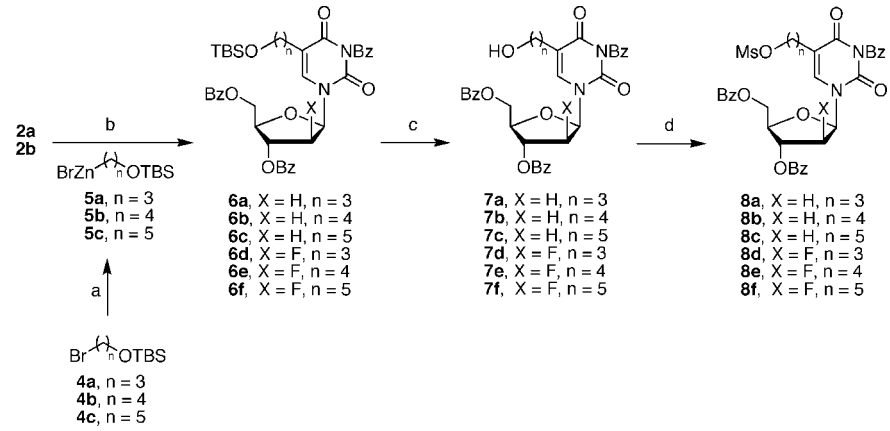

[a] Reagents and conditions: (a) Zn, I_2, DMA, 80 °C; (b) $Pd(P(t\text{-}Bu)_3)_2$, DMA, rt; (c) 1% HCl, EtOH, rt; and (d) MsCl, Et_3N, CH_2Cl_2, 0 °C → rt.

Scheme 3. Radiofluorination of 5-*O*-Mesylate Precursors **8a**−**f** to Afford **[^{18}F]1a**−**f**[a]

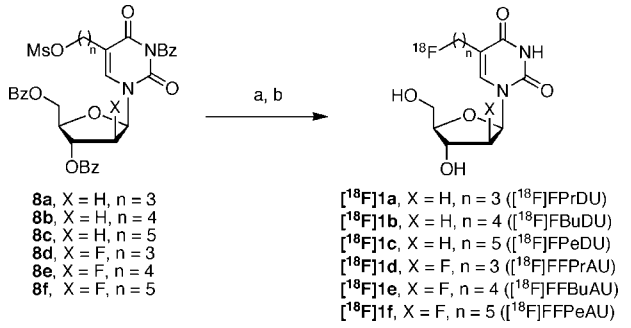

[a] Reagents and conditions: (a) [^{18}F]KF, K[2,2,2], K_2CO_3, DMF, 135 °C, 5 min and (b) 0.5 N NaOMe, MeOH, 135 °C, 5 min.

[^{18}F]3a−**f**. Interestingly, separate treatments of the isolated **[^{18}F]3a**−**f** fraction and the fraction with all of the other unidentified [^{18}F]-labeled products with 0.5 N NaOMe in MeOH at 135 °C for 5 min resulted in only one major radioactive peak with the same retention time. An HPLC coelution with a nonradioactive cold standard confirmed the identity of the peak as that of the fully debenzoylated 5-[^{18}F]fluoroalkyl pyrimidine nucleoside. This suggests that the conditions of the labeling step produced multiple combinations of *N*-, 3′-, and 5′-debenzoylated nucleosides that all had the [^{18}F] radiolabel incorporated at the terminus of the 5-alkyl chain. As a result of this observation, unlike previous reports for the synthesis of 5-[^{18}F]fluoroalkyl pyrimidine nucleosides,[16,24] we did not attempt to isolate the [^{18}F]-labeled tribenzoyl-protected nucleosides **[^{18}F]3a**−**f** from the crude reaction mixture via solid-phase extraction or HPLC. Instead, we immediately heated the reaction mixture at 135 °C for 5 min with 0.5 M NaOMe in MeOH to remove all remaining benzoyl protecting groups. **[^{18}F]1a**−**f** were isolated by solid-phase extraction followed by HPLC purification with an appropriate HPLC solvent system. The purified product had an HPLC retention time that was consistent with the coeluted cold carrier. (An example of a typical HPLC chromatogram is shown in the Supporting Information.)

By following our labeling method, we were able to obtain purified **[^{18}F]1a**−**f** in decay-corrected yields of 17−35% (Table 1). These yields are higher than the 9.5 and <0.2% (decay-corrected) yields that were reported for [^{18}F]FEDU and [^{18}F]FFEAU, respectively. The radiochemical purity was >99%, and the specific activity, as estimated by HPLC, ranged from 18.5 to 925 GBq/μmol (500 to 25000 mCi/μmol) at the end of synthesis (EOS). The total procedure time was 60−70 min, which is a considerable improvement over the synthesis time of ≥180 min that was reported for all other [^{18}F] sugar-labeled nucleosides targeting HSV1-TK.[25−27] It is also an improvement over the 90−120 min of synthesis time that was reported for [^{18}F]FFEAU.[12,16] It is likely that our two-step, one-pot synthesis can be easily adapted for automation to obtain higher radioactive preparations in an even shorter amount of time.

Partition Coefficient. The lipophilicities (log *P*) of the labeled tracers [^{18}F]FPrDU, [^{18}F]FBuDU, [^{18}F]FPeDU, [^{18}F]FFPrAU, [^{18}F]FFBuAU, and [^{18}F]FFPeAU (**[^{18}F]1a**−**f**, respectively) at pH 7.4 were −0.57 ± 0.09, −0.24 ± 0.02, 0.23 ± 0.02, −0.12 ± 0.01, 0.27 ± 0.002, and 0.74 ± 0.01, respectively (Table 1). As expected, in both the 2′-deoxyuridine series (**[^{18}F]1a**−**c**) and the 2′-fluoro-2′-deoxyarabinouridine series (**[^{18}F]1d**−**f**), the log *P* values increased with increasing fluoroalkyl chain length, which indicates increased lipophilicity attributed to additional methylene units. The log *P* values of the 2′-deoxyuridines **[^{18}F]1a**−**c** were all lower than those of their corresponding 2′-fluoro-2′-deoxyarabinouridines **[^{18}F]1d**−**f**. For comparison, the log *P* of [^{125}I]FIAU at pH 7.4 in our system was 0.05 ± 0.01. The log *P* values can often indicate the ability of compounds to diffuse passively across intact cell membranes, including the blood−brain barrier (BBB). In recent years, there has been a drive to find reporter probes that are selectively phosphorylated by HSV1-TK while being able to permeate the BBB to allow for potential imaging of HSV1-*tk* gene expression in gliomas.[28,29] The moderately lipophilic FIAU does not diffuse across the intact BBB.[30] By reason of log *P* values alone, [^{18}F]FFPeAU (**[^{18}F]1f**) would be expected to cross the BBB by passive diffusion more readily than FIAU or our other synthesized nucleosides. However, very recent studies with the fairly lipophilic 5-iodovinyl pyrimidine nucleosides [^{123}I]IVFRU (log *P* = 1.22) and [^{123}I]IVFAU (log *P* = 1.24) demonstrated a very low brain uptake in normal mice.[29] These results demonstrate that the usual relationship between the BBB permeability and the drug lipophilicity does not apply to these compounds.[29] In addition to log *P* = 1−4, the optimal requirements for crossing the BBB include a molecular weight of <400 and a polar surface area (which highly correlates with hydrogen bonding ability) of <90 Å^2.[31] The higher polar surface area of pyrimidine nucleosides (∼100 Å^2)[32] suggests that their capacity for passive BBB diffusion is inherently low. However, the brain uptake is not necessarily limited to passive diffusion. It is well established that nucleosides that target HSV1-TK are substrates for a variety of nucleoside transporters[33−36] found

Table 1. ^{18}F-Labeling Yields, Preparation Times, and log *P* for [^{18}F]**1a**−**f**[a]

compd	RCY (%)[a]	RCP (%)[b]	prepn time (min)	log *P*[c]	*n*[d]
[^{18}F]FPrDU ([^{18}F]**1a**)	21.6 ± 2.4	>99	60	−0.57	3
[^{18}F]FBuDU ([^{18}F]**1b**)	20.8 ± 4.7	>99	60	−0.24	4
[^{18}F]FPeDU ([^{18}F]**1c**)	35.2 ± 2.6	>99	70	0.23	4
[^{18}F]FFPrAU ([^{18}F]**1d**)	19.3 ± 4.9	>99	60	−0.12	3
[^{18}F]FFBuAU ([^{18}F]**1e**)	20.4 ± 3.4	>99	60	0.27	3
[^{18}F]FFPeAU ([^{18}F]**1f**)	17.3 ± 2.3	>99	70	0.74	8

[a] RCY is radiochemical yield, decay-corrected; results are reported as the mean ± SD [b] RCP is radiochemical purity. [c] log *P* = log([1-octanol]/[0.1 M NaH_2PO_4, pH 7.47]) [d] *n* is the number of experiments performed.

on many cellular membranes, including the BBB. The presence of these transporters on the BBB and in neurons, astrocytes, and glia may also play an important role in the reporter-probe accumulation in the brain. As alluded to in recent studies, a driving force, such as a glioma with HSV1-*tk* gene expression, may be required to increase the brain uptake of the radiolabeled pyrimidine nucleosides.[29] However, further in vivo studies are required to illustrate this point.

Biological Evaluations. Cellular Uptake of [^{18}F]1a−f. The cellular uptake of [^{18}F]FPrDU, [^{18}F]FBuDU, [^{18}F]FPeDU, [^{18}F]FFPrAU, [^{18}F]FFBuAU, and [^{18}F]FFPeAU was studied in two glioma cell lines of murine origin. The first cell line is stably transduced with HSV1-*tk* (RG2TK+) and thus features cytosolic HSV1-TK enzyme activity.[37,38] The second cell line is the nontransduced wild-type glioma cell line (RG2) with no HSV1-TK activity but with native TK1 activity. The cellular accumulation of each compound over a period of 2 h in RG2TK+ cells and in RG2 cells is illustrated in Figure 2. All of the [^{18}F] tracers accumulated in RG2TK+ cells in a time-dependent manner, and the uptake was significantly higher than the minimal uptake observed in RG2 cells ($P < 0.006$). [^{18}F]FPrDU and [^{18}F]FBuDU showed the greatest accumulation in RG2TK+ cells ($P < 0.0003$) at 8.4 and 8.3% of the total radioactivity per 10^6 cells, respectively. Whereas the [^{18}F]FPrDU uptake plateaued after 2 h of treatment, the [^{18}F]FBuDU uptake steadily increased, even at 2 h. In comparison, the uptake of [^{125}I]FIAU at 2 h is 29.4% per 10^6 cells. The degree of uptake of the [^{18}F] tracers in RG2TK+ cells at 2 h followed the order of [^{18}F]FBuDU ≅ [^{18}F]FPrDU ≫ [^{18}F]FPeDU ≅ [^{18}F]FFBuAU > [^{18}F]FFPrAU > [^{18}F]FFPeAU.

The sensitivity of the tracers for HSV1-*tk*-expressing cells should depend on the binding affinity of the nucleosides for HSV1-TK and their subsequent phosphorylation rate by the enzyme. Despite the considerable flexibility of the HSV1-TK active site toward C-5 pyrimidine nucleosides, our data suggested a significant decrease in the sensitivity of the viral enzyme toward 2′-fluoro-2′-deoxyarabinouridine nucleosides. This is evidenced by the substantially lower cellular uptake of the 2′-fluoro-2′-deoxyarabinouridines [^{18}F]FFPrAU, [^{18}F]FFBuAU, and [^{18}F]FFPeAU as compared with their 2′-deoxyribose counterparts. Similar observations were reported for studies that compared 5-iodovinyl [^{125}I]IVDU and [^{125}I]IVFAU uptake in KBALB-STK cells expressing HSV1-*tk*, where the 2′-fluorine substituent in the arabino configuration of [^{125}I]IVFAU lowered the cellular accumulation compared with that using [^{125}I]IVDU.[39,40]

Results also suggested that the five-carbon chain of the pyrimidine ring in [^{18}F]FPeDU and [^{18}F]FFPeAU may be too long for the HSV1-TK enzyme P1 subpocket, leading to diminished binding capacity and thus significantly decreased accumulations of phosphorylated products relative to the shorter-chained nucleosides ($0.0007 < P < 0.05$). The uptake was maximal when the carbon chain length was three or four in the 2′-deoxyuridine series and four carbons in the 2′-fluoro-2′-deoxyarabinouridine series. For longer time points, [^{18}F]FBuDU and [^{18}F]FFBuAU, with their four-carbon chain lengths, would apparently lead to the greatest cellular accumulation in HSV1-TK-positive cells. These results were consistent with antiviral-SAR relationships that establish optimal inhibition when the 5-substituent is no longer than four carbons.[41]

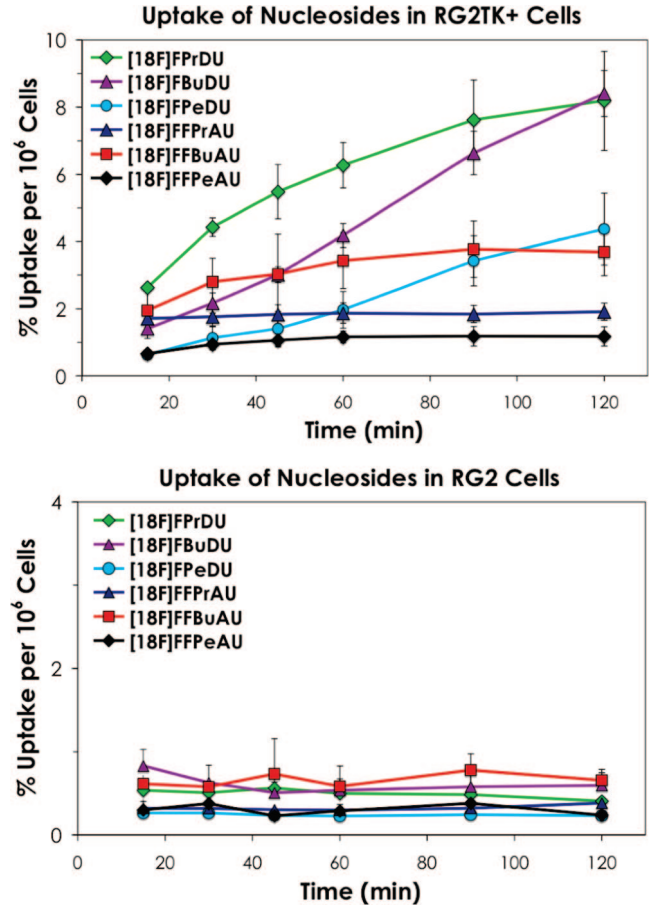

Figure 2. In vitro cellular uptake of [^{18}F]FPrDU, [^{18}F]FBuDU, [^{18}F]FPeDU, [^{18}F]FFPrAU, [^{18}F]FFBuAU, and [^{18}F]FFPeAU ([^{18}F]**1a**−**f**, respectively) in RG2TK+ and RG2 cells. Data are expressed as the mean ± SD of three or more independent experiments performed in duplicate.

An initial screen to assess the binding potential of the nonradioactive nucleosides **1a**−**f** for HSV1-TK was performed in RG2TK+ cells. The in vitro accumulation of [^{125}I]FIAU was monitored in the presence of increasing concentrations of nucleosides **1a**−**f** as inhibitors (Figure 3) to determine the relative strength of these compounds toward inhibiting [^{125}I]FIAU from binding HSV1-TK. (For experimental details, see the Supporting Information.) The [^{125}I]FIAU accumulation in RG2TK+ cells was inhibited by **1a**−**f** with IC_{50} values that ranged from 7.6 ± 0.5 to 36.8 ± 8.3 μM for FPrDU and FPeDU, respectively (Table 2). The 5-fluoroalkyl pyrimidines **1a**−**f** were at least 10 times less sensitive than FIAU (IC_{50} = 0.7 ± 0.09 μM) toward inhibiting [^{125}I]FIAU accumulation. In RG2 cells,

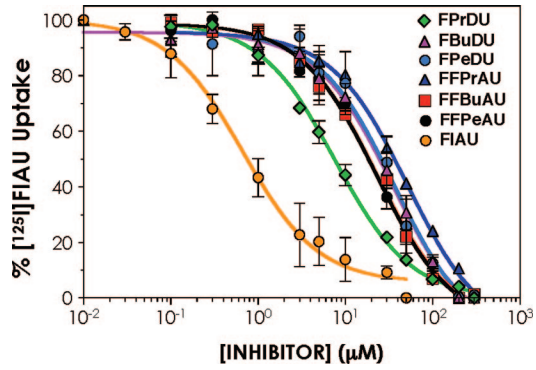

Figure 3. [^{125}I]FIAU accumulation in RG2TK+ cells with increasing concentrations (0−300 μM) of inhibitors FPrDU (**1a**), FBuDU (**1b**), FPeDU (**1c**), FFPrAU (**1d**), FFBuAU (**1e**), and FFPeAU (**1f**) compared with FIAU. Data are expressed as the mean ± SD of three or more independent experiments performed in duplicate.

Table 2. Inhibition of [^{125}I]FIAU Uptake After 2 h of Incubation with 5-Fluoroalkyl Pyrimidine Nucleosides **1a**−**f** in Murine Glioma Cells (RG2TK+)

compd	IC_{50} in RG2TK+ cells[a]
FPrDU, **1a**	7.6 ± 0.5
FBuDU, **1b**	34.5 ± 3.7
FPeDU, **1c**	36.8 ± 8.3
FFPrAU, **1d**	51.2 ± 5.6
FFBuAU, **1e**	23.0 ± 2.0
FFPeAU, **1f**	22.9 ± 1.9
FIAU	0.7 ± 0.1

[a] IC_{50} (μM) is the inhibitory concentration required to inhibit [^{125}I]FIAU uptake by 50%. Results are reported as the mean ± SD of at least three independent experiments performed in duplicate.

where there is only mammalian TK activity, [^{125}I]FIAU accumulation is 10 times lower than in RG2TK+ cells. As such, the relative potencies of **1a**−**f** compared with that of FIAU could not be accurately gauged (data not shown). Nonetheless, no correlation could be found between the results from the uptake inhibition assay using [^{125}I]FIAU with **1a**−**f** and the cellular uptake assays with **[^{18}F]1a**−**f**. Upon further consideration, it is apparent that the net uptake of [^{125}I]FIAU inside RG2TK+ cells reflects not only the enzyme activity of HSV1-TK but also the transport of [^{125}I]FIAU across the cell membrane. Because these new nucleosides have not been evaluated as substrates for nucleoside transporters, we are unsure of which mechanism is predominant in inhibiting the cellular accumulation of [^{125}I]-FIAU. Consequently, this screening assay may not truly reflect the binding potential to HSV1-TK but rather the inhibition of nucleoside transport.

When wild-type RG2 cells were used as a control for nonspecific accumulation, the cellular uptake at 2 h ranged from 0.66 to 0.23% for [^{18}F]FFBuAU and [^{18}F]FPeDU, respectively, and all uptake values were significantly lower than the uptake values in RG2TK+ cells ($P < 0.006$) (Table 3). Comparable to previous reports, there was considerable uptake of [^{125}I]FIAU in RG2 cells that has been attributed to phosphorylation by endogenous mammalian TK1. Furthermore, the [^{125}I]FIAU uptake at 3.44% was significantly higher than that of **[^{18}F]1a**−**f**. The very low uptake of **[^{18}F]1a**−**f** in the control cells suggests that our tracers are not phosphorylated by endogenous mammalian TK. As a result, the background activity of **[^{18}F]1a**−**f** in rapidly proliferating tissue, such as tumor cells, would be very low compared with that of FIAU. This is especially critical when trying to detect lower levels of HSV1-*tk* gene expression.

When developing and comparing tracers for in vivo HSV1-*tk* reporter gene imaging, one must consider the contrast, or

Table 3. Comparison of Cellular Uptake of Tracers after 2 h of Incubation in RG2TK+ and RG2 Cells

	% uptake per 10^6 cells[a]		
compd	RG2TK+	RG2	uptake selectivity index (RGTK+/RG2)
[^{18}F]FPrDU	8.2 ± 1.5	0.41 ± 0.07	20.5 ± 4.4
[^{18}F]FBuDU	8.4 ± 0.7	0.59 ± 0.16	14.9 ± 4.0
[^{18}F]FPeDU	4.4 ± 1.1	0.23 ± 0.07	19.9 ± 6.9
[^{18}F]FFPrAU	1.9 ± 0.3	0.38 ± 0.03	5.0 ± 0.7
[^{18}F]FFBuAU	3.7 ± 0.7	0.66 ± 0.13	7.8 ± 4.3
[^{18}F]FFPeAU	1.2 ± 0.3	0.24 ± 0.01	5.5 ± 2.3
[^{125}I]FIAU	29.4 ± 7.4	3.4 ± 2.0	9.9 ± 4.6

[a] Results are reported as the mean ± SD of at least three independent experiments performed in duplicate.

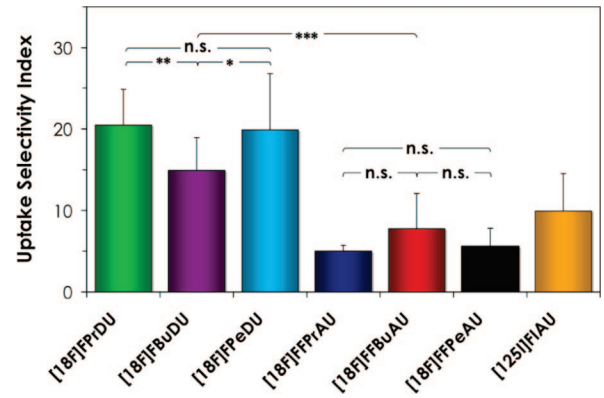

Figure 4. Cellular uptake selectivity index of [^{18}F]FPrDU, [^{18}F]F-BuDU, [^{18}F]FPeDU, [^{18}F]FFPrAU, [^{18}F]FFBuAU, and [^{18}F]FFPeAU (average tracer accumulation ratio between RG2TK+ and RG2 cells). [^{18}F]FPrDU vs [^{18}F]FBuDU, **, $P < 0.007$; [^{18}F]FPrDU vs [^{18}F]F-PeDU, n.s., $P > 0.05$; [^{18}F]FBuDU vs [^{18}F]FPeDU, *, $P < 0.05$; [^{18}F]FBuDU vs [^{18}F]FFBuAU, ***, $P < 0.001$; [^{18}F]FFPrAU vs [^{18}F]FFBuAU, [^{18}F]FFPrAU vs [^{18}F]FFPeAU, and [^{18}F]FFBuAU vs [^{18}F]FFPeAU, n.s., $P > 0.05$; [^{125}I]FIAU vs [^{18}F]FPrDU, FBuDU, and FPeDU, ***, $P < 0.001$; [^{125}I]FIAU vs [^{18}F]FFPrAU, **, $P < 0.005$; [^{125}I]FIAU vs [^{18}F]FFPeAU, *, $P < 0.02$; [^{125}I]FIAU vs [^{18}F]FFPeAU, n.s., $P > 0.05$.

selectivity, between radiotracer uptake in HSV1-*tk* expressing cells and that in HSV1-*tk*-negative cells. The uptake selectivity indices among the six different nucleosides, as determined by taking the average ratio of the tracer accumulation between RG2TK+ and RG2 cells, are shown in Figure 4. In the RG2TK+/RG2 cellular system, the uptake selectivity indexes of [^{18}F]FPrDU and [^{18}F]FPeDU were both significantly higher than that of [^{18}F]FBuDU ($P < 0.0007$ and 0.05, respectively) but were not significantly different from each other ($P > 0.05$) (Figure 4). The selectivity indices of the 2′-fluoro-2′-deoxyarabinouridines [^{18}F]FFPrAU, [^{18}F]FFBuAU, and [^{18}F]FFPeAU were not statistically different from one another ($P > 0.05$). The uptake selectivity indices were on the order of [^{18}F]FPrDU ≅ [^{18}F]FPeDU > [^{18}F]FBuDU ≫ [^{18}F]FFBuAU ≅ [^{18}F]FF-PrAU ≅ [^{18}F]FFPeAU. The selectivity of [^{125}I]FIAU fell between that of the 2′-deoxyuridines and the 2′-fluoro-2′-deoxyarabinouridines (Table 3).

In our experiments, the affinity of the reference tracer [^{125}I]FIAU was relatively high compared with that of our new [^{18}F] tracers. However, FIAU was actively phosphorylated by cellular mammalian TK, which significantly lowered the selectivity index of FIAU. Although our tracers apparently have a lower affinity for HSV1-TK compared with FIAU, they are minimally phosphorylated by mammalian TK. As such, the two series of [^{18}F]-labeled nucleosides, in particular [^{18}F]FPrDU, [^{18}F]FBuDU, [^{18}F]FPeDU, and [^{18}F]FFBuAU, exhibited favor-

Table 4. Cytotoxic Activity of 5-Fluoroalkyl Pyrimidine Nucleosides **1a−f** against Murine Glioma Cells RG2TK+ and RG2 as Determined by MTT Assay[a]

compd	cytotoxic activity (CC_{50})	
	RG2TK+	RG2
FPrDU, **1a**	>1000	>450
FBuDU, **1b**	>800	>800
FPeDU, **1c**	>650	>750
FFPrAU, **1d**	209	121
FFBuAU, **1e**	346	355
FFPeAU, **1f**	375	>1000
GCV	5.86	377
FIAU	0.79	80

[a] CC_{50} (μM) is the cytotoxic concentration required to inhibit cell proliferation by 50%. Results are reported as the mean ± SEM of three independent experiments performed in duplicate.

able HSV1-TK sensitivity and uptake selectivity that would allow for the in vivo imaging of a dynamic range of HSV1-TK expression levels. This would include the detection of lower levels of HSV1-*tk* gene expression in highly proliferating tissues, which is a considerable challenge that has been raised for successful in vivo HSV1-TK imaging using [^{123}I]/[^{124}I]/[^{18}F]FIAU. Therefore, this study shows the potential of [^{18}F]FPrDU, [^{18}F]FBuDU, [^{18}F]FPeDU, and [^{18}F]FFBuAU as novel tracers for HSV1-TK imaging and merits additional studies to assess the in vivo potential of these HSV1-*tk* imaging probes.

Cytotoxic Activity. In view of the fact that the tracers **[^{18}F]1a−f** accumulated selectively in RG2TK+ cells and not in RG2 cells, the nonradioactive nucleosides FPrDU, FBuDU, FPeDU, FFPrAU, FFBuAU, and FFPeAU (**1a−f**, respectively) were evaluated for their antiproliferative activity toward the RG2TK+ and RG2 glioma cells by the use of the MTT assay. The RG2 cell line was used as a negative control to assess the intrinsic cytotoxicity of the nucleosides. Both GCV and FIAU exerted a significant cytotoxic effect to RG2TK+ cells with a CC_{50} of 5.86 and 0.79 μM, respectively (Table 4). This was in stark contrast with **1a−f**, which all exhibited negligible-to-low cytotoxicity to RG2TK+ cells (CC_{50} > 1000−1209 μM). Interestingly, the 2′-fluoro-2′-deoxyarabinouridines **1d−f** were generally more cytotoxic to RG2TK+ cells than the analogous 2′-deoxyuridines **1a−c**; this observation was often made when we compared the two classes of pyrimidine nucleosides for antiviral activity.[42] This is in contrast with our observations for the in vitro uptake assays where the 2′-deoxyuridines **[^{18}F]1a−c** were more active for HSV1-TK-directed phosphorylation. As expected, GCV was not active against RG2 cells. However, FIAU was found to be moderately toxic to RG2 cells. This is indicative of prodrug activation by TK1 and is in agreement with the significant in vitro accumulation of [^{125}I]FIAU in RG2 cells due to phosphorylation by TK1. The toxicity of nucleosides **1a−f** to RG2 cells was the same as or slightly higher than their toxicity to RG2TK+ cells, and a broad correlation between the cytotoxicity and 5-fluoroalkyl chain length was revealed in only RG2 cells.

Nucleosides are almost always prodrugs of metabolically activated phosphate derivatives. Once prodrugs are inside the cell, their activation relies exclusively on the presence of HSV1-TK activity. However, the monophosphate must be further phosphorylated by cellular kinases, and only then is the "active drug" available to bind and inhibit other cellular enzymes. Our results emphasized that although HSV1-TK phosphorylated the 5-fluoroalkyl pyrimidine nucleosides, as evidenced by the intracellular accumulation of [^{18}F]-labeled products, the nucleoside prodrugs were not efficiently processed to the cytotoxic triphosphate species, hence the lower toxicity toward both HSV1-*tk*-expressing cells and nontransduced cells compared with that toward GCV or FIAU.

Summary and Conclusions

In employing the Negishi coupling method that was developed for the synthesis of six 5-fluoroalkylated pyrimidine nucleosides (**1a−f**), we achieved a very short and efficient three-step synthesis of the respective 5-*O*-mesylate precursors for ^{18}F labeling. The radiolabeling method described herein afforded three new 5-[^{18}F]fluoroalkyl-2′-deoxyuridines (**[^{18}F]1a−c**) and three new 2′-fluoro-2′-deoxy-5-[^{18}F]fluoroalkyl arabinouridines (**[^{18}F]1d−f**) in good yields and with very short preparation times. This is more favorable than the previously reported approaches to synthesizing [^{18}F]-labeled pyrimidine nucleosides targeting HSV1-TK. The maximal cellular accumulation of the radiotracers occurs when the 5-alkyl chain length is three to four carbons in both nucleoside series, although 5-(5-[^{18}F]fluoropentyl)-2′-deoxyuridines still accumulate to an appreciable degree in HSV1-TK+ cells. Our results suggest that the 5-alkyl substituent length does not necessarily dictate the sensitivity of radiotracers as PET imaging probes of HSV1-TK. Indeed, the pentose sugar moiety, in our case, a deoxyribose or an arabinose, also plays a critical role in directing the binding potential and the subsequent phosphorylation of these nucleosides by HSV1-TK. Despite the significant accumulation of phosphorylated products of **[^{18}F]1a−f** in HSV1-*tk*-expressing cells, there was negligible cytotoxicity of these compounds to these same cells. Taken together, 5-[^{18}F]fluoropropyl, [^{18}F]fluorobutyl, and [^{18}F]fluoropentyl pyrimidine nucleosides [^{18}F]FPrDU, [^{18}F]FBuDU, [^{18}F]FFBuAU, and [^{18}F]FPeDU exhibit promising in vitro sensitivity and selectivity that makes them candidates for further in vivo evaluations as HSV1-TK-PET probes for HSV1-*tk* reporter gene expression.

Experimental Section

General Information. All commercially available materials were used without further purification unless otherwise indicated. Radioactive [^{125}I]iodide was purchased from Perkin-Elmer Life and Analytical Sciences (Boston, MA) as [^{125}I]NaI (185 MBq (5 mCi) in 0.1 M NaOH, pH 12−14) in no-carrier-added form. [^{18}F]Fluoride was purchased from IBA Molecular (Somerset, NJ) as an [^{18}O]-enriched aqueous solution of [^{18}F]fluoride. Tetrahydrofuran (THF), dichloromethane (DCM), and ether (Et_2O) were dried by a solvent tower (Pure-Solv systems, Innovative Technologies, Newburyport, MA). Unless otherwise indicated, all described reactions were carried out in flame-dried glassware in a dry argon atmosphere. All alkylzinc reagents were prepared according to published procedures,[20,21] and 3-*N*-benzoyl-3′,5′-di-*O*-benzoyl-5-iodo-2′-deoxyuridine[43,44] (**2a**) and 3-*N*-benzoyl-3′,5′-di-*O*-benzoyl-2′-fluoro-2′-deoxy-5-iodo-1-β-D-arabinouridine[45] (**2b**) were prepared according to modified literature protocols.[20,25,46] Ultraviolet spectra were recorded on a Beckman DU-640 spectrophotometer. A Bruker DPX spectrometer was used to record ^{1}H spectra at 200 MHz and ^{13}C NMR spectra at 50 MHz. Whereas ^{1}H and ^{13}C NMR spectra for the 2′-deoxyuridine derivatives were referenced to $CDCl_3$ or CD_3OD, ^{1}H and ^{13}C NMR data for the 2′-deoxy-2′-fluoroarabinouridine derivatives were referenced to CD_3CN. Chemical shifts (δ) are given in parts per million (ppm), and coupling constants are in hertz (Hz). ^{1}H NMR splitting patterns are designated as singlet (s), doublet (d), doublet of doublets (dd), doublet of triplets (dt), doublet of doublet of doublets (ddd), triplet (t), quartet (q), pentet (p), multiplet (m), and broad (br). Unless otherwise indicated, ^{13}C NMR data are recorded as singlet (s). We performed high-resolution mass spectrometry (HRMS) by using an Agilent G3250AA instrument (LC/MSD time-of-flight (TOF)). High-performance liquid chromatography was performed on an Agilent 1100 series system. Two systems were used to confirm the purity of the bioactive compounds

listed in this section: system A (Phenomenex Gemini C_{18} reverse-phase analytical column (4.6 × 250 mm^2, 5 μm), MeOH/H_2O (70:30), flow rate (1 mL/min), 268 nm) and system B (Phenomenex silica normal-phase column (4.6 × 250 mm^2, 10 μm), MeOH/CH_2Cl_2 (10:90), flow rate (1 mL/min), 268 nm). All compounds used for further biological evaluation in this article showed >95% purity in both HPLC systems. Radioactivity was determined by gamma counting (Cobra II auto-gamma counter D5003 spectrometer, Canberra-Packard). We measured ^{125}I counts in the 15−75 keV range and ^{18}F counts in the 400−1600 keV energy range. Solid-phase extraction cartridges Sep-Pak C_{18}, Sep-Pak QMA Light, and Oasis HLB (6 mL) were purchased from Waters (Milford, MA). RG2 cells were obtained from the American Tissue Culture Collection (ATCC), and RG2TK+ cells were a kind gift from Dr. Juri Gelovani. Cell proliferation assays using 3-(4,5-dimethylthiazol-2-yl)-2,5-diphenyltetrazolium bromide (MTT) (Sigma, Milwaukee, WI) were analyzed using a Bio-Rad model 550 microplate reader.

Chemistry. General Procedure A for Deprotection of Bz Moieties. 3-*N*-Benzoyl-3′,5′-di-*O*-benzoyl-5-(5-fluoroalkyl) pyrimidine nucleosides **3a**−**f** were prepared according to an optimized Negishi coupling method that was developed in our laboratory.[20] A 0.5 N NaOMe/MeOH solution (0.5 mL) was added to **3a**−**f** in anhydrous MeOH (2 mL), and the reaction mixture was heated at 80 °C for 15 min with stirring. After the mixture was cooled to room temperature, 1 N HCl (0.25 mL) was added, and the solvent was removed in vacuo. The residue was purified via preparative silica gel TLC (10% MeOH in DCM).

5-(3-Fluoropropyl)-2′-deoxyuridine (FPrDU) (1a). Compound **1a** was prepared from **3a** (14 mg, 0.023 mmol) as a white solid (6 mg, 97%) according to general procedure A. ^{1}H NMR (CD_3OD, δ): 7.87 (s, 1H), 6.28 (t, 1H, J = 6.7 Hz), 4.45 (dt, 2H, J_1 = 5.9, J_2 = 47.4 Hz), 4.39−4.36 (m, 1H), 3.92 (q, 1H, J = 3.3 Hz), 3.78 (dd, 1H, J_1 = 12.0, J_2 = 17.2 Hz), 3.76 (dd, 1H, J_1 = 12.0, J_2 = 17.6 Hz), 2.46−2.39 (m, 2H), 2.28−2.21 (m, 4H), 2.02−1.79 (m, 2H). ^{13}C NMR (CD_3OD, δ): 166.0, 152.4, 138.8, 114.9, 89.1, 86.6, 84.3 (d, J = 163.1 Hz), 72.3, 62.9, 41.5, 30.5 (d, J = 19.7 Hz), 24.1 (d, J = 5.7 Hz). UV (MeOH) λ_{max}, nm (ε): 266 (8400). HRMS (*m*/*z*): [M + Na]$^+$ calcd for $C_{12}H_{17}FN_2O_5Na$, 311.1019; found, 311.1028. HRMS (*m*/*z*): [M + K]$^+$ calcd for $C_{12}H_{17}FN_2O_5K$, 327.0759; found, 327.0765.

5-(4-Fluorobutyl)-2′-deoxyuridine (FBuDU) (1b). Compound **1b**[20] was prepared from **3b** (22 mg, 0.036 mmol) as a white solid (11 mg, >99%) according to general procedure A.^{1}H NMR (CD_3OD, δ): 8.06 (s, 1H), 6.49 (t, 1H, J_1 = 6.7 Hz), 4.64 (dt, 2H, J_1 = 5.6, J_2 = 47.6 Hz), 4.64−4.57 (m, 1H), 4.12 (t, 1H, J_1 = 3.1 Hz), 3.98 (dd, 1H, J_1 = 12.1, J_2 = 16.8 Hz), 3.96 (dd, 1H, J_1 = 12.1, J_2 = 17.3 Hz), 2.59−2.37 (m, 4H), 2.00−1.81 (m, 4H). ^{13}C NMR (CD_3OD, δ): 166.1, 152.4, 138.6, 115.6, 89.1, 86.6, 84.8 (d, J = 162.8 Hz), 72.4, 62.9, 41.5, 31.2 (d, J = 19.6 Hz), 27.5, 25.6 (d, J = 5.1 Hz). UV (MeOH) λ_{max}, nm (ε): 266 (10 400). HRMS (*m*/*z*): [M + H]$^+$ calcd for $C_{13}H_{20}FN_2O_5$, 303.1356; found, 303.1349.

5-(5-Fluoropentyl)-2′-deoxyuridine (FPeDU) (1c). Compound **1c** was prepared from **3c** (14 mg, 0.022 mmol) as a white solid (6 mg, 85%) according to general procedure A. ^{1}H NMR (CD_3OD, δ): 7.85 (s, 1H), 6.29 (t, 1H, J_1 = 6.7 Hz), 4.42 (dt, 2H, J_1 = 6.0, J_2 = 47.5 Hz), 4.44−4.37 (m, 1H), 4.12 (q, 1H, J_1 = 3.2 Hz), 3.77 (dd, 1H, J_1 = 12.1, J_2 = 16.8 Hz), 3.76 (dd, 1H, J_1 = 12.0, J_2 = 17.3 Hz), 2.36−2.20 (m, 4H), 1.84−1.34 (m, 6H). ^{13}C NMR (CD_3OD, δ): 166.2, 152.4, 138.5, 115.8, 89.1, 86.5, 84.9 (d, J = 162.4 Hz), 72.4, 63.0, 41.5, 31.4 (d, J = 19.6 Hz), 29.3, 27.8, 26.0 (d, J = 5.4 Hz). UV (MeOH) λ_{max}, nm (ε): 267 (10 100). HRMS (*m*/*z*): [M + H]$^+$ calcd for $C_{14}H_{22}FN_2O_5$, 315.1513; found, 317.1502.

2′-Fluoro-2′-deoxy-5-(3-fluoropropyl)-1-β-D-arabinofuranosyluracil (FFPrAU) (1d). Compound **1d** was prepared from **3d** (14 mg, 0.023 mmol) as a white solid (7 mg, >99%) according to general procedure A. ^{1}H NMR (CD_3CN, δ): 9.08 (bs, 1H), 7.53 (s, 1H), 6.14 (dd, 1H, J_1 = 4.2, J_2 = 15.7 Hz), 5.02 (dt, 1H, J_1 = 3.9, J_2 = 52.5 Hz), 4.44 (dt, 2H, J_1 = 5.9, J_2 = 47.4 Hz), 4.40−4.23 (m, 1H), 4.12 (t, 1H, J_1 = 3.1 Hz), 3.88−3.70 (m, 3H), 2.41−2.33 (m, 2H), 1.91−1.71 (m, 2H). ^{13}C NMR (CD_3CN, δ): 138.9, 96.8 (d, J = 190.5 Hz), 84.4 (d, J = 161.1 Hz), 84.6 (d, J = 4.8 Hz), 84.1 (d, J = 16.7 Hz), 74.4 (d, J = 24.6 Hz), 61.5, 30.1 (d, J = 19.5 Hz), 23.6 (d, J = 5.6 Hz). UV (MeOH) λ_{max}, nm (ε): 266 (2000). HRMS (*m*/*z*): [M + Na]$^+$calcd for $C_{12}H_{16}F_2N_2O_5Na$, 329.0925; found, 329.0925. HRMS (*m*/*z*): [M + K]$^+$ calcd for $C_{12}H_{16}F_2N_2O_5K$, 345.0664; found, 345.0664.

2′-Fluoro-2′-deoxy-5-(4-fluorobutyl)-1-β-D-arabinofuranosyluracil (FFBuAU) (1e). Compound **1e**[20] was prepared from **3e** (13 mg, 0.021 mmol) as a white solid (6 mg, 95%) according to general procedure A.^{1}H NMR (CD_3CN with D_2O, δ): 7.53 (s, 1H), 6.13 (dd, 1H, J_1 = 4.1, J_2 = 16.4 Hz), 5.02 (dt, 2H, J_1 = 3.9, J_2 = 52.2 Hz), 4.43 (dt, 2H, J_1 = 5.9, J_2 = 47.3 Hz), 4.24−4.20 (m, 1H), 3.90−3.70 (m, 3H), 2.32−2.25 (m, 2H), 1.78−1.45 (m, 4H). ^{13}C NMR (CD_3CN, δ): 164.2, 151.2, 138.0 (d, J = 3.0 Hz), 114.2, 96.8 (d, J = 190.4 Hz), 85.0 (d, J = 160.7 Hz), 84.5 (d, J = 4.6 Hz), 84.0 (d, J = 16.6 Hz), 74.4 (d, J = 24.5 Hz), 61.5, 30.6 (d, J = 19.4 Hz), 27.1, 25.0 (d, J = 5.4 Hz). UV (MeOH) λ_{max}, nm (ε): 265 (8800). HRMS (*m*/*z*): [M + H]$^+$ calcd for $C_{13}H_{19}F_2N_2O_5$, 321.1262; found, 321.1253.

2′-Fluoro-2′-deoxy-5-(5-fluoropentyl)-1-β-D-arabinofuranosyluracil (FFPeAU) (1f). Compound **1f** was prepared from **3f** (30 mg, 0.046 mmol) as a white solid (15 mg, 99%) according to general procedure A. ^{1}H NMR (CD_3CN with D_2O, δ): 7.91 (s, 1H), 6.13 (dd, 1H, J_1 = 4.1, J_2 = 16.5 Hz), 5.03 (dt, 2H, J_1 = 3.5, J_2 = 52.2 Hz), 4.41 (dt, 2H, J_1 = 6.1, J_2 = 47.4 Hz), 4.24−4.20 (m, 1H), 3.91−3.63 (m, 3H), 2.29−2.22 (m, 2H), 1.79−1.30 (m, 6H). ^{13}C NMR (CD_3CN, δ): 164.3, 151.2, 137.9 (d, J = 2.9 Hz), 114.5, 96.8 (d, J = 190.4 Hz), 85.2 (d, J = 160.6 Hz), 84.5 (d, J = 4.7 Hz), 84.0 (d, J = 16.7 Hz), 74.4 (d, J = 24.5 Hz), 61.6, 30.9 (d, J = 19.2 Hz), 28.9, 27.4, 25.4 (d, J = 5.7 Hz). UV (MeOH) λ_{max}, nm (ε): 265 (10 200). HRMS (*m*/*z*): [M + H]$^+$ calcd for $C_{14}H_{21}F_2N_2O_5$, 335.1419; found, 335.1419.

General Procedure B for the Preparation of 5-*O*-TBS-Protected Nucleosides via Negishi Cross Coupling. To a flame-dried 5 mL two-neck flask equipped with a stir bar were added **2a** (300 mg, 0.45 mmol) or **2b** (308 mg, 0.45 mmol), Pd(P(*t*-Bu)$_3$)$_2$ (11.5 mg, 0.023 mmol), and anhydrous DMA (5 mL) under argon. To the reaction mixture, alkylzinc reagents **5a**−**c**[20,21] (0.7−0.8 M solution in DMA, 1.35 mmol) were added dropwise, and the reaction was stirred at room temperature for 30 min. The reaction mixture was quenched with saturated NH_4Cl (10 mL) and was extracted with EtOAc (3 × 5 mL). The combined organic phases were washed with brine, dried over $MgSO_4$, filtered, and concentrated. We purified the crude product mixture by silica gel chromatography using 20−30% EtOAc in hexanes to yield a white solid.

3-*N*-Benzoyl-3′,5′-di-*O*-benzoyl-5-(3-tert-butyldimethylsilyloxypropyl)-2′-deoxyuridine (6a). Compound **6a**[20] was prepared from **2a** and (3-*tert*-butyldimethylsilyloxypropyl)zinc bromide **5a** (1.93 mL of 0.7 M solution in DMA) as a white solid in 45% yield according to general procedure B. ^{1}H NMR ($CDCl_3$, δ): 8.09−7.90 (m, 6H), 7.69−7.42 (m, 9H), 7.40 (s, 1H), 6.43 (dd, 1H, J_1 = 5.4, J_2 = 8.7 Hz), 5.67−5.64 (m, 1H), 4.77 (dd, 1H, J_1 = 12.2, J_2 = 14.4 Hz), 4.75 (dd, 1H, J_1 = 12.2, J_2 = 14.6 Hz), 4.59−4.55 (m, 1H), 3.51 (t, 2H, J = 6.2 Hz), 2.77 (ddd, 1H, J_1 = 1.4, J_2 = 5.4, J_3 = 14.2 Hz), 2.40 (ddd, 1H, J_1 = 6.6, J_2 = 8.6, J_3 = 14.4 Hz), 2.30−2.19 (m, 2H), 1.66−1.52 (m, 2H), 0.88 (s, 9H), 0.03 (s, 6H). ^{13}C NMR ($CDCl_3$, δ): 169.0, 166.2, 162.4, 149.4, 135.2, 134.4, 134.0, 133.9, 131.9, 130.7, 130.0, 129.8, 129.6, 129.4, 129.2, 129.0, 128.8, 115.9, 85.8, 83.1, 75.2, 64.5, 62.6, 38.3, 31.6, 26.2, 24.1, 18.5, −5.1. HRMS (*m*/*z*): [M + Na]$^+$ calcd for $C_{39}H_{44}N_2O_9SiNa$, 735.2174; found, 735.2688. HRMS (*m*/*z*): [M + H]$^+$ calcd for $C_{39}H_{45}N_2O_9Si$, 713.2894; found, 713.2881.

3-*N*-Benzoyl-3′,5′-di-*O*-benzoyl-5-(4-tert-butyldimethylsilyloxybutyl)-2′-deoxyuridine (6b). Compound **6b** was prepared from **2a** and (4-*tert*-butyldimethylsilyloxybutyl)zinc bromide **5b** (1.69 mL of 0.8 M solution in DMA) as a white solid (122 mg, 38% yield) according to general procedure B. ^{1}H NMR ($CDCl_3$, δ): 8.09−7.89 (m, 6H), 7.69−7.43 (m, 9H), 7.35 (s, 1H), 6.45 (dd, 1H, J_1 = 5.4, J_2 = 8.6 Hz), 5.69−5.66 (m, 1H), 4.77 (dd, 1H, J_1

= 12.2, J_2 = 23.0 Hz), 4.76 (dd, 1H, J_1 = 12.2, J_2 = 23.5 Hz), 4.59−4.56 (m, 1H), 3.55−3.49 (m, 2H), 2.77 (ddd, 1H, J_1 = 1.4, J_2 = 5.5, J_3 = 14.1 Hz), 2.40 (ddd, 1H, J_1 = 6.6, J_2 = 8.6, J_3 = 14.3 Hz), 2.13−2.06 (m, 2H), 1.42−1.40 (m, 4H), 0.89 (s, 9H), 0.04 (s, 6H). ^{13}C NMR ($CDCl_3$, δ): 168.9, 166.2, 162.4, 149.4, 135.2, 134.4, 134.0, 131.9, 130.6, 130.0, 129.8, 129.4, 129.1, 128.8, 116.2, 85.6, 83.1, 75.2, 64.5, 63.0, 38.3, 32.7, 27.2, 26.2, 25.2, 23.2, −5.0. HRMS (*m*/*z*): $[M + Na]^+$ calcd for $C_{40}H_{46}N_2O_9SiNa$, 749.2870; found,749.2901. HRMS (*m*/*z*): $[M + H]^+$ calcd for $C_{40}H_{47}N_2O_9Si$, 727.3051; found,727.3128.

3-*N*-Benzoyl-3′,5′-di-*O*-benzoyl-5-(5-tert-butyldimethylsilyloxypentyl)-2′-deoxyuridine (6c). Compound **6c** was prepared from **2a** and (5-*tert*-butyldimethylsilyloxypentyl)zinc bromide **5c** (1.90 mL of 0.72 M solution in DMA) as a white solid (144 mg, 43% yield) according to general procedure B. ^{1}H NMR ($CDCl_3$, δ): 8.10−7.89 (m, 6H), 7.69−7.42 (m, 9H), 7.34 (s, 1H), 6.46 (dd, 1H, J_1 = 5.4, J_2 = 8.8 Hz), 5.70−5.67 (m, 1H), 4.79 (dd, 1H, J_1 = 12.2, J_2 = 28.1 Hz), 4.76 (dd, 1H, J_1 = 12.2, J_2 = 28.7 Hz), 4.59−4.55 (m, 1H), 3.55 (t, 2H, J = 6.4 Hz), 2.77 (ddd, 1H, J_1 = 1.2, J_2 = 5.5, J_3 = 14.3 Hz), 2.40 (ddd, 1H, J_1 = 6.3, J_2 = 8.5, J_3 = 14.5 Hz), 2.17−1.96 (m, 2H), 1.49−1.15 (m, 6H), 0.90 (s, 9H), 0.05 (s, 6H). ^{13}C NMR ($CDCl_3$, δ): 169.0, 166.2, 162.4, 149.4, 135.2, 134.2, 134.0, 131.9, 130.6, 130.0, 129.8, 129.6, 129.4, 129.2, 129.1, 128.8, 116.4, 85.5, 83.1, 75.2, 64.5, 63.3, 38.3, 32.7, 28.7, 27.4, 26.2, 25.9, 26.2, 18.6, −5.0. HRMS (*m*/*z*): $[M + Na]^+$ calcd for $C_{41}H_{48}N_2O_9SiNa$, 763.3027; found, 763.3014. HRMS (*m*/*z*): $[M + H]^+$ calcd for $C_{41}H_{49}N_2O_9Si$, 741.3207; found, 741.3200.

3-*N*-Benzoyl-3′,5′-di-*O*-benzoyl-2′-fluoro-2′-deoxy-5-(3-tert-butyldimethylsilyloxypropyl)-1-β-D-arabinofuranosyluracil (6d). Compound **6d** was prepared from **2b** and (3-*tert*-butyldimethylsilyloxypropyl)zinc bromide **5a** (1.93 mL of 0.7 M solution in DMA) as a white solid in 38% yield according to general procedure B. ^{1}H NMR (CD_3CN, δ): 8.11−7.93 (m, 6H), 7.75−7.47 (m, 10H), 6.30 (dd, 1H, J_1 = 3.2, J_2 = 20.7 Hz), 5.67 (ddd, 1H, J_1 = 1.0, J_2 = 3.6, J_3 = 19.2 Hz), 5.44 (ddd, 1H, J_1 = 1.0, J_2 = 3.1, J_3 = 50.3 Hz), 4.78 (dd, 1H, J_1 = 12.1, J_2 = 21.4 Hz), 4.76 (dd, 1H, J_1 = 12.1, J_2 = 22.3 Hz), 4.61 (q, 1H, J = 3.8 Hz), 3.53 (t, 2H, J = 6.2 Hz), 2.29−2.22 (m, 2H), 1.63−1.50 (m, 2H), 0.86 (s, 9H), 0.01 (s, 6H). ^{13}C NMR (CD_3CN, δ): 170.4, 167.1, 166.4, 163.5, 150.1, 137.9, 137.8, 136.5, 135.0, 134.6, 132.7, 131.4, 130.8, 130.6, 130.5, 130.1, 129.8, 114.9, 94.4 (d, J = 189.8 Hz), 85.7 (d, J = 16.4 Hz), 81.4, 77.8 (d, J = 30.3 Hz), 64.3, 63.1, 32.3, 26.4, 24.3, 19.0, −5.0. HRMS (*m*/*z*): $[M + Na]^+$ calculated for $C_{39}H_{43}FN_2O_9SiNa$, 753.2620; found, 753.2639. HRMS (*m*/*z*): $[M + H]^+$ calcd for $C_{39}H_{44}FN_2O_9Si$, 731.2800; found, 731.2865.

3-*N*-Benzoyl-3′,5′-di-*O*-benzoyl-2′-fluoro-2′-deoxy-5-(4-tert-butyldimethylsilyloxybutyl)-1-β-D-arabinofuranosyluracil (6e). Compound **6e** was prepared from **2b** and (4-*tert*-butyldimethylsilyloxybutyl)zinc bromide **5b** (1.69 mL of 0.8 M solution in DMA) as a white solid (95 mg, 29% yield) according to general procedure B: ^{1}H NMR (CD_3CN, δ): 8.12−7.90 (m, 6H), 7.79−7.48 (m, 10H), 6.36 (dd, 1H, J_1 = 3.2, J_2 = 20.8 Hz), 5.68 (ddd, 1H, J_1 = 1.0, J_2 = 3.8, J_3 = 19.0 Hz), 5.44 (ddd, 1H, J_1 = 1.0, J_2 = 3.3, J_3 = 50.4 Hz), 4.78 (dd, 1H, J_1 = 12.1, J_2 = 25.7 Hz), 4.76 (dd, 1H, J_1 = 12.5, J_2 = 27.0 Hz), 4.64−4.59 (m, 1H), 3.54 (t, 2H, J = 6.0 Hz), 2.18−2.05 (m, 2H), 1.42−1.32 (m, 4H), 0.86 (s, 9H), 0.01 (s, 6H). ^{13}C NMR (CD_3CN, δ): 170.4, 167.1, 166.4, 163.5, 150.1, 138.0, 137.9, 136.5, 135.0, 134.6, 133.8, 132.6, 131.3, 130.8, 130.5, 129.85, 129.82, 129.8, 115.1, 94.5 (d, J = 189.7 Hz), 85.6 (d, J = 16.5 Hz), 81.4, 77.8 (d, J = 30.2 Hz), 64.3, 63.6, 33.1, 27.4, 26.4, 25.8, 19.0, −5.0. HRMS (*m*/*z*): $[M + Na]^+$ calcd for $C_{40}H_{45}FN_2O_9SiNa$, 767.2776; found, 767.2796. HRMS (*m*/*z*): $[M + H]^+$ calcd for $C_{40}H_{46}FN_2O_9Si$, 745.2957; found, 745.3015.

3-*N*-Benzoyl-3′,5′-di-*O*-benzoyl-2′-fluoro-2′-deoxy-5-(5-tert-butyldimethylsilyloxypentyl)-1-β-D-arabinofuranosyluracil (6f). Compound **6f** was prepared from **2b** and (5-*tert*-butyldimethylsilyloxypentyl)zinc bromide **5c** (1.90 mL of 0.72 M solution in DMA) as a white solid (131 mg, 38% yield) according to general procedure B. ^{1}H NMR (CD_3CN, δ): 8.11−7.92 (m, 6H), 7.77−7.48 (m, 10H), 6.30 (dd, 1H, J_1 = 3.2, J_2 = 20.7 Hz), 5.68 (dd, 1H, J_1 = 3.5, J_2 = 18.9 Hz), 5.43 (dd, 1H, J_1 = 3.2, J_2 = 50.3 Hz), 4.77 (dd, 1H, J_1 = 12.1, J_2 = 28.1 Hz), 4.75 (dd, 1H, J_1 = 12.1, J_2 = 29.5 Hz), 4.63−4.57 (m, 1H), 3.54 (t, 2H, J = 6.1 Hz), 2.21−2.11 (m, 2H), 1.46−1.18 (m, 6H), 0.87 (s, 9H), 0.02 (s, 6H). ^{13}C NMR (CD_3CN, δ): 170.4, 167.1, 166.4, 163.5, 150.1, 137.9, 137.86, 136.5, 135.0, 134.6, 132.6, 131.1, 130.8, 130.58, 130.55, 130.53, 129.84, 129.81, 129.80, 115.2, 94.4 (d, J = 189.7 Hz), 85.6 (d, J = 16.4 Hz), 81.4, 77.8 (d, J = 30.3 Hz), 64.2, 63.8, 33.4, 29.2, 27.6, 26.4, 26.1, 19.0, −5.0. HRMS (*m*/*z*): $[M + Na]^+$ calcd for $C_{41}H_{47}FN_2O_9SiNa$, 781.2933; found, 781.2977. HRMS (*m*/*z*): $[M + H]^+$ calcd for $C_{41}H_{48}FN_2O_9Si$, 759.3113; found, 759.3170.

General Procedure C for Deprotection of *O*-TBS Moiety. A solution of 1% concentrated HCl in EtOH (5 mL) was added to the *O*-TBS-protected nucleosides **6a**−**f** and stirred for 10 min at room temperature.[47] To the reaction mixture, 0.25 M NaOH in EtOH (5 mL) was added. The solvent was removed in vacuo, and the residue was purified by silica gel chromatography (10% MeOH in DCM) to afford a white solid.

3-*N*-Benzoyl-3′,5′-di-*O*-benzoyl-5-(3-hydroxypropyl)-2′-deoxyuridine (7a). Compound **7a** was prepared from **6a** (144 mg, 0.2 mmol) as a white solid (121 mg, >99%) according to general procedure C. ^{1}H NMR ($CDCl_3$, δ): 8.10−7.89 (m, 6H), 7.69−7.44 (m, 10H), 6.45 (dd, 1H, J_1 = 5.4, J_2 = 8.7 Hz), 5.69−5.66 (m, 1H), 4.79 (dd, 1H, J_1 = 12.2, J_2 = 25.0 Hz), 4.77 (dd, 1H, J_1 = 12.2, J_2 = 26.0 Hz), 4.60−4.57 (m, 1H), 3.49 (t, 2H, J = 5.9 Hz), 2.77 (dd, 1H, J_1 = 5.1, J_2 = 13.9 Hz), 2.39 (ddd, 1H, J_1 = 6.6, J_2 = 8.5, J_3 = 14.5 Hz), 2.30−2.13 (m, 2H), 1.64−1.51 (m, 2H). ^{13}C NMR ($CDCl_3$, δ): 168.8, 166.4, 166.3, 163.1, 149.4, 135.3, 133.9, 131.6, 130.6, 129.91, 129.90, 129.7, 129.5, 129.4, 129.1, 129.0, 128.8, 128.7, 115.4, 85.7, 83.2, 75.1, 64.5, 61.2, 38.4, 32.0, 23.2. HRMS (*m*/*z*): $[M + Na]^+$ calcd for $C_{33}H_{30}N_2O_9Na$, 621.1849; found, 621.1878. HRMS (*m*/*z*): $[M + H]^+$ calcd for $C_{33}H_{31}N_2O_9$, 599.2030; found, 599.2036.

3-*N*-Benzoyl-3′,5′-di-*O*-benzoyl-5-(4-hydroxybutyl)-2′-deoxyuridine (7b). Compound **7b** was prepared from **6b** (119 mg, 0.16 mmol) as a white solid (100 mg, >99%) according to general procedure C. ^{1}H NMR ($CDCl_3$, δ): 8.10−7.83 (m, 6H), 7.69−7.43 (m, 9H), 7.39 (s, 1H), 6.46 (dd, 1H, J_1 = 5.4, J_2 = 8.7 Hz), 5.69−5.66 (m, 1H), 4.78 (dd, 1H, J_1 = 12.2, J_2 = 26.5 Hz), 4.77 (dd, 1H, J_1 = 12.2, J_2 = 27.4 Hz), 4.60−4.57 (m, 1H), 3.61−3.55 (m, 2H), 2.52 (ddd, 1H, J_1 = 1.2, J_2 = 5.5, J_3 = 14.1 Hz), 2.47−2.33 (m, 1H), 2.16−2.10 (m, 2H), 1.48−1.45 (m, 4H). ^{13}C NMR ($CDCl_3$, δ): 168.9, 166.3, 166.2, 162.5, 149.4, 135.3, 134.5, 134.0, 132.3, 131.8, 130.6, 130.0, 129.8, 129.6, 129.4, 129.2, 129.1, 129.8, 115.9, 85.6, 83.1, 75.1, 64.6, 62.6, 38.3, 32.1, 26.8, 24.9. HRMS (*m*/*z*): $[M + Na]^+$ calcd for $C_{34}H_{32}N_2O_9Na$, 635.2006; found, 635.2038. HRMS (*m*/*z*): $[M + H]^+$ calcd for $C_{34}H_{33}N_2O_9$, 613.2186; found, 613.2211.

3-*N*-Benzoyl-3′,5′-di-*O*-benzoyl-5-(5-hydroxypentyl)-2′-deoxyuridine (7c). Compound **7c** was prepared from **6c** (139 mg, 0.19 mmol) as a white solid (115 mg, 98%) according to general procedure C. ^{1}H NMR ($CDCl_3$, δ): 8.10−7.90 (m, 6H), 7.70−7.43 (m, 9H), 7.35 (s, 1H), 6.47 (dd, 1H, J_1 = 5.5, J_2 = 8.8 Hz), 5.70−5.67 (m, 1H), 4.78 (dd, 1H, J_1 = 12.2, J_2 = 31.5 Hz), 4.76 (dd, 1H, J_1 = 12.2, J_2 = 32.3 Hz), 4.59−4.55 (m, 1H), 3.60 (t, 2H, J = 6.3 Hz), 2.78 (ddd, 1H, J_1 = 1.4, J_2 = 5.5, J_3 = 14.2 Hz), 2.49−2.34 (m, 1H), 2.23−1.97 (m, 2H), 1.55−1.16 (m, 4H). ^{13}C NMR ($CDCl_3$, δ): 169.0, 166.2, 162.4, 149.4, 135.2, 134.4, 134.0, 131.9, 130.6, 130.0, 129.9, 129.5, 129.4, 129.2, 129.1, 128.8, 116.1, 85.5, 83.0, 75.2, 64.6, 62.9, 38.3, 32.4, 28.4, 27.1, 25.5. HRMS (*m*/*z*): $[M + Na]^+$ calcd for $C_{35}H_{34}N_2O_9Na$, 649.2162; found, 649.2167. HRMS (*m*/*z*): $[M + H]^+$ calcd for $C_{35}H_{35}N_2O_9$, 627.2343; found, 627.2383.

3-*N*-Benzoyl-3′,5′-di-*O*-benzoyl-2′-fluoro-2′-deoxy-5-(3-hydroxypropyl)-1-β-D-arabinofuranosyluracil (7d). Compound **7d** was prepared from **6d** (117 mg, 0.16 mmol) as a white solid (89 mg, 90%) according to general procedure C. ^{1}H NMR (CD_3CN, δ): 8.12−7.94 (m, 6H), 7.79−7.48 (m, 10H), 6.30 (dd, 1H, J_1 = 3.2, J_2 = 20.7 Hz), 5.68 (ddd, 1H, J_1 = 0.8, J_2 = 3.6, J_3 = 19.0 Hz), 5.44 (ddd, 1H, J_1 = 0.8, J_2 = 3.1, J_3 = 50.4 Hz), 4.79 (dd, 1H, J_1 = 12.2, J_2 = 23.9 Hz), 4.77 (dd, 1H, J_1 = 12.2, J_2 = 25.2 Hz), 4.64−4.58 (m, 1H), 3.46−3.37 (m, 2H), 2.54 (t, 1H, J = 5.4

Hz), 2.29−2.22 (m, 2H), 1.62−1.48 (m, 2H). ^{13}C NMR (CD_3CN, δ): 170.4, 167.2, 166.4, 163.7, 150.1, 138.2, 138.1, 136.5, 135.0, 134.6, 132.6, 131.4, 130.8, 130.6, 130.5, 130.1, 129.84, 129.82, 114.9, 94.9 (d, J = 189.8 Hz), 85.6 (d, J = 16.4 Hz), 81.4, 77.6 (d, J = 30.2 Hz), 64.3, 61.7, 32.4, 24.1. HRMS (*m*/*z*): $[M + Na]^+$ calcd for $C_{33}H_{29}FN_2O_9Na$, 639.1755; found, 639.1757. HRMS (*m*/*z*): $[M + H]^+$ calcd for $C_{33}H_{30}FN_2O_9$, 617.1935; found, 617.1944.

3-*N*-Benzoyl-3′,5′-di-*O*-benzoyl-2′-fluoro-2′-deoxy-5-(4-hydroxybutyl)-1-β-D-arabinofuranosyluracil (7e). Compound **7e** was prepared from **6e** (183 mg, 0.25 mmol) as a white solid (137 mg, 87%) according to general procedure C. ^{1}H NMR (CD_3CN, δ): 8.13−7.91 (m, 6H), 7.79−7.48 (m, 10H), 6.31 (dd, 1H, J_1 = 3.2, J_2 = 20.8 Hz), 5.69 (ddd, 1H, J_1 = 0.9, J_2 = 3.6, J_3 = 19.0 Hz), 5.44 (ddd, 1H, J_1 = 1.0, J_2 = 3.2, J_3 = 50.2 Hz), 4.79 (dd, 1H, J_1 = 12.1, J_2 = 27.7 Hz), 4.77 (dd, 1H, J_1 = 12.1, J_2 = 29.0 Hz), 4.64−4.58 (m, 1H), 3.46−3.34 (m, 2H), 2.43 (t, 1H, J = 5.4 Hz), 2.25−2.15 (m, 2H), 1.43−1.32 (m, 4H). ^{13}C NMR (CD_3CN, δ): 170.5, 167.1, 166.4, 163.5, 150.1, 138.1, 138.0, 136.5, 135.0, 134.6, 133.9, 132.6, 131.4, 130.8, 130.5, 129.9, 129.8, 115.1, 94.5 (d, J = 189.8 Hz), 85.6 (d, J = 16.3 Hz), 81.4, 77.9 (d, J = 30.2 Hz), 64.2, 62.3, 33.0, 27.4, 25.8. HRMS (*m*/*z*): $[M + Na]^+$ calcd for $C_{34}H_{31}FN_2O_9Na$, 653.1911; found, 653.1924. HRMS (*m*/*z*): $[M + H]^+$ calcd for $C_{34}H_{32}FN_2O_9$, 631.2092; found, 631.2122.

3-*N*-Benzoyl-3′,5′-di-*O*-benzoyl-2′-fluoro-2′-deoxy-5-(5-hydroxypentyl)-1-β-D-arabinofuranosyluracil (7f). Compound **7f** was prepared from **6f** (86 mg, 0.11 mmol) as a white solid (71 mg, >99%) according to general procedure C. ^{1}H NMR (CD_3CN, δ): 8.13−7.93 (m, 6H), 7.79−7.48 (m, 10H), 6.31 (dd, 1H, J_1 = 3.2, J_2 = 20.8 Hz), 5.69 (ddd, 1H, J_1 = 1.0, J_2 = 3.4, J_3 = 19.1 Hz), 5.44 (ddd, 1H, J_1 = 1.0, J_2 = 3.4, J_3 = 50.4 Hz), 4.79 (dd, 1H, J_1 = 12.0, J_2 = 30.8 Hz), 4.77 (dd, 1H, J_1 = 12.0, J_2 = 32.3 Hz), 4.64−4.59 (m, 1H), 3.47−3.38 (m, 2H), 2.41 (t, 1H, J = 5.4 Hz), 2.22−2.15 (m, 2H), 1.46−1.14 (m, 6H). ^{13}C NMR (CD_3CN, δ): 170.5, 168.2, 166.4, 163.5, 150.1, 138.0, 137.8, 136.5, 135.0, 134.6, 132.7, 131.6, 130.8, 130.5, 129.9, 129.8, 115.2, 94.5 (d, J = 190.1 Hz), 85.6 (d, J = 16.7 Hz), 81.4, 77.8 (d, J = 30.2 Hz), 64.2, 62.6, 33.3, 29.2, 27.6, 26.2. HRMS (*m*/*z*): $[M + Na]^+$ calcd for $C_{35}H_{33}FN_2O_9Na$, 667.2068; found, 667.2072. HRMS (*m*/*z*): $[M + H]^+$ calcd for $C_{35}H_{34}FN_2O_9$, 645.2248; found, 645.2255.

General Procedure D for Mesylation of Alcohols. 3-*N*-Benzoyl-3′,5′-di-*O*-benzoyl-5-(3-methanesulfonyloxypropyl)-2′-deoxyuridine (8a). To a stirred solution of **7a** (36 mg, 0.06 mmol) and Et_3N (9 μL, 0.07 mmol) in DCM (5 mL) was added methanesulfonyl chloride (5 μL, 0.7 mmol) at 0 °C in argon. The temperature was maintained at 0 °C for 10 min, the ice bath was removed, and stirring was continued at room temperature for 2.5 h. The reaction mixture was diluted with saturated NH_4Cl and Et_2O, and the organics were washed with NH_4Cl and brine. The organic phase was dried with Na_2SO_4 and was concentrated in vacuo. Silica gel chromatography (10% MeOH in DCM) afforded **8a**[20] as a white solid (33 mg, 81%). ^{1}H NMR (200 MHz, $CDCl_3$, δ): 8.11−7.91 (m, 6H), 7.67−7.43 (m, 10H), 6.46 (dd, 1H, J_1 = 5.5, J_2 = 8.7 Hz), 5.68−5.65 (m, 1H), 4.79 (dd, 1H, J_1 = 12.1, J_2 = 17.1 Hz), 4.78 (dd, 1H, J_1 = 12.1, J_2 = 17.9 Hz), 4.60−4.57 (m, 1H), 4.14 (t, 2H, J = 5.8 Hz), 3.00 (s, 3H), 2.76 (ddd, 1H, J_1 = 1.4, J_2 = 5.4, J_3 = 14.4 Hz), 2.47 (ddd, 1H, J_1 = 6.7, J_2 = 8.6, J_3 = 14.3 Hz), 2.31 (t, 2H, J = 7.2 Hz), 1.94−1.81 (m, 2H). ^{13}C NMR (50 MHz, $CDCl_3$, δ): 168.8, 166.3, 166.2, 162.4, 149.4, 136.1, 135.3, 133.9, 131.7, 130.7, 130.0, 129.8, 129.7, 129.4, 129.2, 129.1, 128.8, 113.7, 85.7, 83.2, 75.1, 68.8, 64.4, 38.1, 37.7, 27.5, 23.9. HRMS (*m*/*z*): $[M + Na]^+$ calcd for $C_{34}H_{32}N_2O_{11}SNa$, 699.1625; found, 699.1604.

3-*N*-Benzoyl-3′,5′-di-*O*-benzoyl-5-(4-methanesulfonyloxybutyl)-2′-deoxyuridine (8b). Compound **8b** was prepared from alcohol **7b** (91 mg, 0.15 mmol) as a white solid (85 mg, 83%) according to general procedure D. ^{1}H NMR ($CDCl_3$, δ): 8.10−7.89 (m, 6H), 7.71−7.40 (m, 10H), 6.46 (dd, 1H, J_1 = 5.4, J_2 = 8.7 Hz), 5.70−5.67 (m, 1H), 4.79 (dd, 1H, J_1 = 12.2, J_2 = 31.5 Hz), 4.77 (dd, 1H, J_1 = 12.1, J_2 = 32.4 Hz), 4.60−4.55 (m, 1H), 4.15 (t, 2H, J = 6.2 Hz), 3.00 (s, 3H), 2.78 (ddd, 1H, J_1 = 1.2, J_2 = 5.5, J_3 = 14.2 Hz), 2.49−2.34 (m, 1H), 2.16−2.09 (m, 2H), 1.65−1.44 (m, 4H). ^{13}C NMR ($CDCl_3$, δ): 168.9, 166.2, 162.4, 149.4, 135.3, 135.0, 134.1, 134.0, 131.8, 130.6, 130.0, 129.8, 129.6, 129.4, 129.2, 129.1, 129.8, 115.3, 85.7, 83.2, 75.2, 69.6, 64.5, 38.3, 37.6, 28.8, 26.7, 24.8. HRMS (*m*/*z*): $[M + Na]^+$ calcd for $C_{35}H_{34}N_2O_{11}SNa$, 713.1781; found, 713.1772. HRMS (*m*/*z*): $[M + H]^+$ calcd for $C_{35}H_{35}N_2O_{11}S$, 691.1962; found, 691.1952.

3-*N*-Benzoyl-3′,5′-di-*O*-benzoyl-5-(5-methanesulfonyloxypentyl)-2′-deoxyuridine (8c). Compound **8c** was prepared from alcohol **7c** (89 mg, 0.14 mmol) as a white solid (91 mg, 91%) according to general procedure D. ^{1}H NMR ($CDCl_3$, δ): 8.10−7.90 (m, 6H), 7.70−7.43 (m, 9H), 7.37 (s, 1H), 6.47 (dd, 1H, J_1 = 5.5, J_2 = 8.5 Hz), 5.70−5.67 (m, 1H), 4.78 (dd, 1H, J_1 = 12.1, J_2 = 33.2 Hz), 4.77 (dd, 1H, J_1 = 12.1, J_2 = 34.3 Hz), 4.62−4.52 (m, 1H), 4.17 (t, 2H, J = 6.3 Hz), 3.00 (s, 3H), 2.78 (dd, 1H, J_1 = 5.0, J_2 = 14.3 Hz), 2.49−2.34 (m, 1H), 2.16−2.05 (m, 2H), 1.69−1.59 (m, 2H), 1.32−1.27 (m, 4H). ^{13}C NMR ($CDCl_3$, δ): 168.9, 166.2, 162.4, 149.4, 135.3, 134.6, 134.1, 134.0, 131.8, 130.6, 130.0, 129.8, 129.4, 129.1, 128.8, 115.7, 85.6, 83.1, 75.2, 70.1, 64.6, 38.3, 37.6, 28.8, 28.1,27.1, 25.2. HRMS (*m*/*z*): $[M + Na]^+$ calcd for $C_{36}H_{36}N_2O_{11}SNa$, 727.1938; found, 727.1921. HRMS (*m*/*z*): $[M + H]^+$ calcd for $C_{36}H_{37}N_2O_{11}S$, 705.2118; found, 705.2107.

3-*N*-Benzoyl-3′,5′-di-*O*-benzoyl-2′-fluoro-2′-deoxy-5-(3-methanesulfonyloxy-propyl)-1-β-D-arabinofuranosyl uracil (8d). Compound **8d** was prepared from alcohol **7d** (42 mg, 0.067 mmol) as a white solid (46 mg, 99%) according to general procedure D. ^{1}H NMR (CD_3CN, δ): 8.13−7.95 (m, 6H), 7.79−7.47 (m, 10H), 6.31 (dd, 1H, J_1 = 3.2, J_2 = 20.6 Hz), 5.69 (ddd, 1H, J_1 = 1.0, J_2 = 3.8, J_3 = 18.8 Hz), 5.45 (ddd, 1H, J_1 = 1.0, J_2 = 3.3, J_3 = 44.0 Hz), 4.79 (dd, 1H, J_1 = 12.1, J_2 = 22.9 Hz), 4.77 (dd, 1H, J_1 = 12.1, J_2 = 24.1 Hz), 4.65−4.59 (m, 1H), 4.13 (t, 2H, J = 6.2 Hz), 2.97 (s, 3H), 2.36−2.27 (m, 2H), 1.89−1.75 (m, 2H). ^{13}C NMR (CD_3CN, δ): 170.3, 167.1, 166.3, 163.4, 150.1, 138.65, 138.57, 136.6, 134.9, 134.6, 132.6, 131.4, 130.9, 130.8, 130.7, 130.6, 130.5, 130.1, 129.9, 129.8, 113.7, 94.4 (d, J = 189.8 Hz), 85.7 (d, J = 16.4 Hz), 81.5 (d, J = 1.3 Hz), 77.8 (d, J = 30.2 Hz), 70.9, 64.3, 37.5, 28.7, 24.1. HRMS (*m*/*z*): $[M + Na]^+$ calcd for $C_{34}H_{31}FN_2O_{11}SNa$, 717.1530; found, 717.1527. HRMS (*m*/*z*): $[M + H]^+$ calcd for $C_{34}H_{32}FN_2O_{11}S$, 695.1711; found, 695.1709.

3-*N*-Benzoyl-3′,5′-di-*O*-benzoyl-2′-fluoro-2′-deoxy-5-(4-methanesulfonyloxybutyl)-1-β-D-arabinofuranosyl uracil (8e). Compound **8e** was prepared from alcohol **7e** (134 mg, 0.21 mmol) as a white solid (127 mg, 84%) according to general procedure D. ^{1}H NMR (CD_3CN, δ): 8.12−7.93 (m, 6H), 7.79−7.48 (m, 10H), 6.31 (dd,1H, J_1 = 3.2, J_2 = 20.7 Hz), 5.69 (dd, 1H, J_1 = 3.1, J_2 = 19.0 Hz), 5.44 (ddd, 1H, J_1 = 1.0, J_2 = 3.2, J_3 = 50.3 Hz), 4.79 (dd, 1H, J_1 = 12.1, J_2 = 29.7 Hz), 4.77 (dd, 1H, J_1 = 12.1, J_2 = 31.0 Hz), 4.64−4.58 (m, 1H), 4.12 (t, 2H, J = 5.4 Hz), 2.97 (s, 3H), 2.32−2.15 (m, 2H), 1.65−1.38 (m, 4H). ^{13}C NMR (CD_3CN, δ): 170.4, 167.1, 166.4, 163.5, 150.1, 136.1, 135.3, 133.9, 132.6, 131.7, 130.7, 130.0, 129.8, 129.7, 129.4, 129.2, 129.1, 128.8, 114.6, 94.5 (d, J = 189.9 Hz), 85.6 (d, J = 16.4 Hz), 81.5, 77.8 (d, J = 30.3 Hz), 71.5, 64.3, 37.5, 29.2, 27.1, 25.4. HRMS (*m*/*z*): $[M + Na]^+$ calcd for $C_{35}H_{33}FN_2O_{11}SNa$, 731.1687; found, 731.1681. HRMS (*m*/*z*): $[M + H]^+$ calcd for $C_{35}H_{34}FN_2O_{11}S$, 709.1817; found, 709.1897.

3-*N*-Benzoyl-3′,5′-di-*O*-benzoyl-2′-fluoro-2′-deoxy-5-(5-methanesulfonyloxy-pentyl)-1-β-D-arabinofuranosyl uracil (8f). Compound **8f** was prepared from alcohol **7f** (110 mg, 0.18 mmol) as a white solid (111 mg, 89%) according to general procedure D. ^{1}H NMR (CD_3CN, δ): 8.18−7.93 (m, 6H), 7.79−7.48 (m, 10H), 6.30 (dd, 1H, J_1 = 3.3, J_2 = 20.7 Hz), 5.70 (ddd, 1H, J_1 = 0.8, J_2 = 3.5, J_3 = 19.1 Hz), 5.44 (ddd, 1H, J_1 = 0.9, J_2 = 3.3, J_3 = 50.2 Hz), 4.79 (dd, 1H, J_1 = 12.1, J_2 = 32.4 Hz), 4.77 (dd, 1H, J_1 = 12.1, J_2 = 33.8 Hz), 4.64−4.59 (m, 1H), 4.13 (t, 2H, J = 6.4 Hz), 2.98 (s, 3H), 2.22−2.12 (m, 2H), 1.69−1.55 (m, 2H), 1.47−1.23 (m, 4H). ^{13}C NMR (CD_3CN, δ): 170.4, 167.1, 166.4, 163.5, 150.1, 138.1, 138.0, 136.5, 135.0, 134.7, 132.6, 131.3, 130.8, 130.5, 130.1, 129.9, 129.8, 114.9, 94.5 (d, J = 189.8 Hz), 85.6 (d, J = 16.3 Hz), 81.4, 77.8 (d, J = 30.3 Hz), 71.7, 64.2, 37.4, 29.5, 28.7, 27.3, 25.6. HRMS (*m*/*z*): $[M + Na]^+$ calcd for $C_{36}H_{35}FN_2O_{11}SNa$, 745.1843;

found, 745.1833. HRMS (*m/z*): $[M + H]^+$ calcd for $C_{36}H_{36}FN_2O_{11}S$, 723.2024; found,723.2018.

Radiochemistry. General Procedure for the Preparation of 2′-Fluoro-2′-deoxy-5-[^{125}I]iodo-1-β-D-arabinofuranosyluracil ([^{125}I]FIAU). [^{125}I]FIAU was prepared by the iododestannylation method as previously reported.[48] Briefly, to a solution of 5-tri-*n*-butylstannyl derivative of FIAU (100 μg, 0.19 μmol) in MeOH (50 μL) was added [^{125}I]NaI (18.5−37 MBq (0.5−1 mCi) in 0.1 M NaOH solution, pH 12−14), followed by the addition of 30% H_2O_2/acetic acid (1:3, v/v) (25 μL). The reaction was vortex mixed and left at room temperature for 30 min. Saturated sodium bisulfite solution (0.1 mL) was added to quench the reaction, followed by saturated sodium bicarbonate (0.2 mL). The reaction mixture was loaded onto a Sep-Pak C_{18} cartridge (preconditioned with 5 mL of EtOH followed by 10 mL of H_2O). The C_{18} cartridge was eluted with water (3 × 10 mL), followed by MeOH (5 mL) to isolate [^{125}I]FIAU. The methanol was evaporated under a stream of N_2, and the [^{125}I]FIAU was reformulated in MeOH/H_2O (2:8) (100 μL) and purified by HPLC (Phenomenex Gemini C18 analytical column (4.6 × 250 mm^2, 5 μm), MeOH/H_2O (2:8), flow rate 1 mL/min, t_R = 8.2 min). The radiolabeled product was isolated in 74−83% radiochemical yield (RCY) (radiochemical purities (RCP) > 99%). [^{125}I]FIAU was prepared under a no-carrier-added condition, thus any ^{127}I products formed are below the detection limit of the UV spectrophotometer. As such, we assume that the specific activity (SA) of [^{125}I]FIAU is close to the theoretical maximum value of 81.4 × 10^4 GBq/mmol (2200 Ci/mmol) for ^{125}I.

General Procedure for the [^{18}F] Radiolabeling of 5-*O*-Mesylate Precursors 8a−f. [^{18}F]Fluoride was passed through a Sep-Pak Light QMA cartridge (preconditioned with 10 mL of $NaHCO_3$ followed by 10 mL of H_2O), and the cartridge was dried by N_2 flow. The ^{18}F activity was eluted with 1.2 mL of a K[2,2,2]/K_2CO_3 solution (22 mg K[2,2,2] and 4.6 mg K_2CO_3 in CH_3CN/H_2O (1.77/0.23)). The solvent was removed at 120 °C under an N_2 stream. The residue was azeotropically dried with 1 mL of anhydrous CH_3CN twice at 120 °C under an N_2 stream. The ^{18}F-activity was redissolved in anhydrous DMF (0.2 mL) and transferred to a borosilicate glass vial, and the solution was preheated for 30 s in an oil bath set at 135 °C. A solution of the 5-*O*-mesylate precursor **8a−f** (1 to 2 mg) in anhydrous DMF (0.15 mL) was added to the reaction vessel containing the ^{18}F. The reaction was heated at 135 °C for 5 min. To the cooled reaction mixture, anhydrous MeOH (0.1 mL) was added, followed by anhydrous 0.5 N NaOMe/MeOH (0.05 mL), and the mixture was heated at 135 °C for 5 min. The reaction was neutralized with 10% HCl (0.1 mL). Water (10 mL) was added, and the solution was passed through an Oasis HLB (6 mL) cartidge (preconditioned with 10 mL of EtOH, followed by 10 mL of H_2O). The cartridge was washed with water (2 × 5 mL), and the radiolabeled compound was eluted with MeOH (5 mL). The solvent was removed at 120 °C under an N_2 stream, and the residue was reconstituted in MeOH/H_2O (3:7). The compound was purified by HPLC (Phenomenex Gemini C_{18} semipreparative column (10 × 250 mm^2, 5 μm), 268 nm, MeOH/H_2O (3:7) for compounds **[^{18}F]1a−b, d−e** or MeOH/H_2O (4:6) for compounds **[^{18}F]1c** and **1f**, flow rate 2−4 mL/min, t_R = 10.5−23.3 min). The isolated RCY was 17.3−35.2%. To determine the RCP and SA of the HPLC-purified materials, we employed analytical HPLC (Phenomenex Gemini C_{18} analytical column (4.6 × 250 mm^2, 5 μm), 268 nm, MeOH/H_2O (3:7) for compounds **[^{18}F]1a−b, d−e** or MeOH/H_2O (4:6) for compounds **[^{18}F]1c** and **1f**, flow rate 1 mL/min, t_R = 6.0−21.6 min). We estimated the SA by comparing the UV peak intensity of the purified [^{18}F]-labeled compound with the calibration curve for the nonradioactive standard of known concentration.

1-Octanol/Water Partition Coefficient. We determined partition coefficients for [^{125}I]FIAU or 5-[^{18}F]fluoroalkyl nucleosides **[^{18}F]1a−f** by measuring the distribution of the radiolabeled compound in 1-octanol and buffer (0.1 M NaH_2PO_4, pH 7.4). A 20 μL sample of radiolabeled nucleoside (in water) was added to a glass vial containing 3 g each of 1-octanol and buffer. The vial was vortexed for 3 min at room temperature, followed by centrifugation for 5 min to allow for complete separation of the two layers. Two weighed samples (0.5 g each) from the 1-octanol and buffer layers were then counted on a gamma counter. Samples of the 1-octanol layer were repartitioned until consistent partition coefficient values were obtained. The measurements were made in triplicate and were repeated three times. We determined the partition coefficient by calculating the ratio of counts (cpm) per unit weight of the 1-octanol layer to that of the buffer layer. We calculated log *P* values by using the equation

$$\log P = \log\left(\frac{\text{cpm/(g of 1-octanol)}}{\text{cpm/(g of buffer)}}\right)$$

Biology. Cell Culture. Rat glioma cells (RG2) expressing the HSV1-*tk* gene (RG2TK+) were used for these studies, as previously reported.[37,38,48] Nontransduced (wild-type) RG2 cell were used as controls. Cells were cultivated in Dulbecco's modified Eagle's medium (DMEM) supplemented with 10% fetal bovine serum (FBS) and 1% penicillin/streptomycin. RG2TK+ cells were additionally given 250 mg/L G418 for HSV1-*tk*+ cell selection. Cells were incubated at 37 °C under 5% CO_2 and were subcultured by trypsinization using 0.25% trypsin−EDTA.

In Vitro Cell-Uptake Studies of Radiolabeled Nucleosides. RG2TK+ and RG2 cells were seeded at 5 × 10^5 cells/well in 12-well tissue culture plates. After 24 h of incubation at 37 °C, monolayers had grown. Cells were washed twice with warmed phosphate-buffered saline (PBS) solution (2 × 1 mL) and were incubated with 0.5 mL of serum-free media containing approximately 0.02 MBq (0.5 μCi) of [^{125}I]FIAU (SA ≈ 81.4 × 10^4 GBq/mmol, 2200 Ci/mmol) or approximately 0.2 MBq (5 μCi) of [^{18}F]FPrDU, [^{18}F]FFPrAU, [^{18}F]FBuDU, [^{18}F]FFBuAU, [^{18}F]FPeDU, or [^{18}F]FFPeAU (SA ≈ 18.5−925 GBq/μmol, 500−25000 mCi/μmol). Nucleoside accumulation experiments were run for 5, 15, 30, 60, 90, and 120 min at 37 °C. After incubation, the cell culture medium was quickly removed, and the monolayers were washed three times with cold PBS. The cells were released from the culture plates with 0.25% trypsin−EDTA (250 μL/well), and trypsin was neutralized with the cell culture medium (350 μL/well). A 50 μL sample was taken and mixed with 50 μL of Trypan blue so that we could count the number of viable cells. The cell-associated radioactivity was measured by a gamma counter and was normalized to the number of viable cells and to the total activity administered. Results are expressed as the percentage of radioactivity accumulated per 10^6 cells. Each value represents the mean ± SD of three or more independent experiments, and each independent experiment was performed in duplicate.

Cytotoxicity Assays. RG2TK+ and RG2 cells were seeded in a 96-well plate at a density of 1.5 × 10^3 cells/well and were left to incubate overnight at 37 °C. Cells were treated with increasing concentrations of drug in culture media (0.001−1000 μmol/L, 100 μL/well) in quadruplicate. Control groups consisted of cells in media without chemical treatment, and blank wells contained media but no cells. All wells were processed identically and were simultaneously incubated with the treated groups. After incubation for 72 h at 37 °C, MTT solution (20 μL/well of 1 mg/mL) was added to each well, and the cells incubated for 3 h. After this time, the medium was rapidly removed and the formazen crystals that were produced by viable cells were solubilized using DMSO (100 μL/well). The plates were optically scanned at 490 nm (650 nm reference wavelength). Absorbance readings were subtracted from the value of the blank wells. The reduction of cell growth was expressed as a percentage of the control group. Data are expressed as the mean of three independent experiments ± SEM.

Statistical Analysis. Descriptive statistics of the differences in the cellular accumulation of the tracers were calculated using univariate analysis with GraphPad Prism 4.0 and Microsoft Excel 2004. Group data were compared using ANOVA analysis and a two-sided unpaired Student's *t* test; statistical significance was set at $P < 0.05$.

Acknowledgment. The RG2TK+ rat glioma cell line was kindly provided by Dr. Juri Gelovani (Memorial Sloan-

Kettering). We thank Dr. Karl Ploessl for LC-HRMS analysis and Dr. Mercedes Lioni (Wistar Cancer Institute) for assistance with the MTT assay. This work was supported by a grant from the National Institutes of Health (R21-EB-005242) to H.F.K.

Supporting Information Available: Procedures to synthesize some intermediates, ^{1}H and ^{13}C NMR spectra of all bioassayed compounds, HPLC purity analysis for all bioassayed compounds in two different HPLC systems, typical radio-HPLC chromatogram, procedure for cell uptake inhibition, and cell growth inhibition profile. This material is available free of charge via the Internet at http://pubs.acs.org.

References

(1) Serganova, I.; Ponomarev, V.; Blasberg, R. Human reporter genes: potential use in clinical studies. *Nucl. Med. Biol.* **2007**, *34*, 791–807.

(2) De Clercq, E. Antivirals and antiviral strategies. *Nat. Rev. Microbiol.* **2004**, *2*, 704–720.

(3) De Clercq, E.; Andrei, G.; Snoeck, R.; De Bolle, L.; Naesens, L.; Degrève, B.; Balzarini, J.; Zhang, Y.; Schols, D.; Leyssen, P.; Ying, C.; Neyts, J. Acyclic/carbocyclic guanosine analogues as anti-herpesvirus agents. *Nucleosides, Nucleotides Nucleic Acids* **2001**, *20*, 271–285.

(4) Arnér, E. S.; Eriksson, S. Mammalian deoxyribonucleoside kinases. *Pharmacol. Ther.* **1995**, *67*, 155–186.

(5) Knecht, W.; Petersen, G. E.; Munch-Petersen, B.; Piškur, J. Deoxyribonucleoside kinases belonging to the thymidine kinase 2 (TK2)-like group vary significantly in substrate specificity, kinetics and feedback regulation. *J. Mol. Biol.* **2002**, *315*, 529–540.

(6) Furman, P. A.; McGuirt, P. V.; Keller, P. M.; Fyfe, J. A.; Elion, G. B. Inhibition by acyclovir of cell growth and DNA synthesis of cells biochemically transformed with herpesvirus genetic information. *Virology* **1980**, *102*, 420–430.

(7) Pope, I. M.; Poston, G. J.; Kinsella, A. R. The role of the bystander effect in suicide gene therapy. *Eur. J. Cancer* **1997**, *33*, 1005–1016.

(8) Prusoff, W. H. Synthesis and biological activities of iododeoxyuridine, an analog of thymidine. *Biochim. Biophys. Acta* **1959**, *32*, 295–296.

(9) Tjuvajev, J. G.; Avril, N.; Oku, T.; Sasajima, T.; Miyagawa, T.; Joshi, R.; Safer, M.; Beattie, B.; DiResta, G.; Daghighian, F.; Augensen, F.; Koutcher, J.; Zweit, J.; Humm, J.; Larson, S. M.; Finn, R.; Blasberg, R. Imaging herpes virus thymidine kinase gene transfer and expression by positron emission tomography. *Cancer Res.* **1998**, *58*, 4333–4341.

(10) Yaghoubi, S. S.; Couto, M. A.; Chen, C.-C.; Polavaram, L.; Cui, G.; Sen, L.; Gambhir, S. S. Preclinical safety evaluation of ^{18}F-FHBG: a PET reporter probe for imaging herpes simplex virus type 1 thymidine kinase (HSV1-tk) or mutant HSV1-sr39tk's expression. *J. Nucl. Med.* **2006**, *47*, 706–715.

(11) Min, J.-J.; Iyer, M.; Gambhir, S. S. Comparison of [^{18}F]FHBG and [^{14}C]FIAU for imaging of HSV1-tk reporter gene expression: adenoviral infection vs stable transfection. *Eur. J. Nucl. Med. Mol. Imaging* **2003**, *30*, 1547–1560.

(12) Miyagawa, T.; Gogiberidze, G.; Serganova, I.; Cai, S.; Balatoni, J. A.; Thaler, H. T.; Ageyeva, L.; Pillarsetty, N.; Finn, R. D.; Blasberg, R. G. Imaging of HSV-tk reporter gene expression: comparison between [^{18}F]FEAU, [^{18}F]FFEAU, and other imaging probes. *J. Nucl. Med.* **2008**, *49*, 637–648.

(13) Serganova, I.; Doubrovin, M.; Vider, J.; Ponomarev, V.; Soghomonyan, S.; Beresten, T.; Ageyeva, L.; Serganov, A.; Cai, S.; Balatoni, J.; Blasberg, R.; Gelovani, J. Molecular imaging of temporal dynamics and spatial heterogeneity of hypoxia-inducible factor-1 signal transduction activity in tumors in living mice. *Cancer Res.* **2004**, *64*, 6101–6108.

(14) Alauddin, M. M.; Shahinian, A.; Park, R.; Tohme, M.; Fissekis, J. D.; Conti, P. S. In vivo evaluation of 2′-deoxy-2′-[^{18}F]fluoro-5-iodo-1-β-D-arabinofuranosyluracil ([^{18}F]FIAU) and 2′-deoxy-2′-[^{18}F]fluoro-5-ethyl-1-β-D-arabinofuranosyluracil ([^{18}F]FEAU) as markers for suicide gene expression. *Eur. J. Nucl. Med. Mol. Imaging* **2007**, *34*, 822–829.

(15) Chin, F. T.; Namavari, M.; Levi, J.; Subbarayan, M.; Ray, P.; Chen, X.; Gambhir, S. S. Semiautomated radiosynthesis and biological evaluation of [^{18}F]FEAU: a novel PET imaging agent for HSV1-tk/sr39tk reporter gene expression. *Mol. Imaging Biol.* **2008**, *10*, 82–91.

(16) Balatoni, J. A.; Doubrovin, M.; Ageyeva, L.; Pillarsetty, N.; Finn, R. D.; Gelovani, J. G.; Blasberg, R. G. Imaging herpes viral thymidine kinase-1 reporter gene expression with a new ^{18}F-labeled probe: 2′-fluoro-2′-deoxy-5-[^{18}F]fluoroethyl-1-β-D-arabinofuranosyl uracil. *Nucl. Med. Biol.* **2005**, *32*, 811–819.

(17) Wild, K.; Bohner, T.; Folkers, G.; Schulz, G. E. The structures of thymidine kinase from herpes simplex virus type 1 in complex with substrates and a substrate analogue. *Protein Sci.* **1997**, *6*, 2097–2106.

(18) Champness, J. N.; Bennett, M. S.; Wien, F.; Visse, R.; Summers, W. C.; Herdewijn, P.; de Clerq, E.; Ostrowski, T.; Jarvest, R. L.; Sanderson, M. R. Exploring the active site of herpes simplex virus type-1 thymidine kinase by X-ray crystallography of complexes with aciclovir and other ligands. *Proteins* **1998**, *32*, 350–361.

(19) De Winter, H.; Herdewijn, P. Understanding the binding of 5-substituted 2′-deoxyuridine substrates to thymidine kinase of herpes simplex virus type-1. *J. Med. Chem.* **1996**, *39*, 4727–4737.

(20) Chacko, A.-M.; Qu, W.; Kung, H. F. Synthesis of 5-fluoroalkylated pyrimidine nucleosides via Negishi cross-coupling. *J. Org. Chem.* **2008**, *73*, 4874–4881.

(21) Huo, S. Highly efficient, general procedure for the preparation of alkylzinc reagents from unactivated alkyl bromides and chlorides. *Org. Lett.* **2003**, *5*, 423–425.

(22) Cox, D. P.; Terpinski, J.; Lawrynowicz, W. "Anhydrous" tetrabutylammonium fluoride: a mild but highly efficient source of nucleophilic fluoride ion. *J. Org. Chem.* **1984**, *49*, 3216–3219.

(23) Yu, C.-S.; Oberdorfer, F. Synthesis of 4-O-methyl-protected 5-(2-hydroxyethyl)-2′-deoxyuridine derivatives and their nucleophilic fluorination to 5-(2-fluoroethyl)-2′-deoxyuridine. *Synthesis* **1999**, 2057–2064.

(24) Yu, C.-S.; Eisenbarth, J.; Runz, A.; Weber, K.; Zeisler, S.; Oberdorfer, F. Syntheses of 5-(2-radiohaloethyl)- and 5-(2-radiohalovinyl)-2′-deoxyuridines. Novel types of radiotracer for monitoring cancer gene therapy with PET. *J. Labelled Compds. Radiopharm.* **2003**, *46*, 421–439.

(25) Alauddin, M. M.; Conti, P. S.; Fissekis, J. D.; Watanabe, K. A. Synthesis of 2′-deoxy-2′-fluoro-1-β-D-arabinofuranosyl uracil derivatives: a method suitable for preparation of [^{18}F]-labeled nucleosides. *Synth. Commun.* **2002**, *32*, 1757–1764.

(26) Alauddin, M. M.; Conti, P. S.; Fissekis, J. D. A general synthesis of 2′-deoxy-2′-[^{18}F]fluoro-1-β-D-arabinofuranosyluracil and its 5-substituted nucleosides. *J. Labelled Compds. Radiopharm.* **2003**, *46*, 285–289.

(27) Alauddin, M. M.; Conti, P. S.; Fissekis, J. D. Synthesis of [^{18}F]-labeled 2′-deoxy-2′-fluoro-5-methyl-1-β-D-arabinofuranosyluracil ([^{18}F]-FMAU). *J. Labelled Compds. Radiopharm.* **2002**, *45*, 583–590.

(28) Pillarsetty, N.; Cai, S.; Ageyeva, L.; Finn, R. D.; Blasberg, R. G. Synthesis and evaluation of [^{18}F] labeled pyrimidine nucleosides for positron emission tomography imaging of herpes simplex virus 1 thymidine kinase gene expression. *J. Med. Chem.* **2006**, *49*, 5377–5381.

(29) Li, H.-F.; Winkeler, A.; Moharram, S.; Knaus, E. E.; Dittmar, K.; Stöckle, M.; Heiss, W. D.; Wiebe, L. I.; Jacob, A. J. In vivo evaluation of the uptake of [^{123}I]FIAU, [^{123}I]IVFRU and [^{123}I]IVFAU by normal mouse brain: potential for noninvasive assessment of HSV-1 thymidine kinase gene expression in gliomas. *Nucleosides, Nucleotides Nucleic Acids* **2008**, *27*, 57–66.

(30) Jacobs, A.; Bräunlich, I.; Graf, R.; Lercher, M.; Sakaki, T.; Voges, J.; Hesselmann, V.; Brandau, W.; Wienhard, K.; Heiss, W.-D. Quantitative kinetics of [^{124}I]FIAU in cat and man. *J. Nucl. Med.* **2001**, *42*, 467–475.

(31) van de Waterbeemd, H.; Camenisch, G.; Folkers, G.; Chrétien, J. R.; Raevsky, O. A. Estimation of blood-brain barrier crossing of drugs using molecular size and shape, and H-bonding descriptors. *J. Drug Targeting* **1998**, *6*, 151–165.

(32) Ertl, P.; Rohde, B.; Selzer, P. Fast calculation of molecular polar surface area as a sum of fragment-based contributions and its application to the prediction of drug transport properties. *J. Med. Chem.* **2000**, *43*, 3714–3717.

(33) Baldwin, S. A.; Beal, P. R.; Yao, S. Y. M.; King, A. E.; Cass, C. E.; Young, J. D. The equilibrative nucleoside transporter family, SLC29. *Pfluegers Arch.* **2004**, *447*, 735–743.

(34) Hyde, R. J.; Cass, C. E.; Young, J. D.; Baldwin, S. A. The ENT family of eukaryote nucleoside and nucleobase transporters: recent advances in the investigation of structure/function relationships and the identification of novel isoforms. *Mol. Membr. Biol.* **2001**, *18*, 53–63.

(35) Gray, J. H.; Owen, R. P.; Giacomini, K. M. The concentrative nucleoside transporter family, SLC28. *Pflugers Arch.* **2004**, *447*, 728–734.

(36) Ritzel, M. W. L.; Ng, A. M. L.; Yao, S. Y. M.; Graham, K.; Loewen, S. K.; Smith, K. M.; Hyde, R. J.; Karpinski, E.; Cass, C. E.; Baldwin, S. A.; Young, J. D. Recent molecular advances in studies of the concentrative Na^{+}-dependent nucleoside transporter (CNT) family: identification and characterization of novel human and mouse proteins (hCNT3 and mCNT3) broadly selective for purine and pyrimidine nucleosides (system cib). *Mol. Membr. Biol.* **2001**, *18*, 65–72.

(37) Tjuvajev, J. G.; Stockhammer, G.; Desai, R.; Uehara, H.; Watanabe, K.; Gansbacher, B.; Blasberg, R. G. Imaging the expression of transfected genes in vivo. *Cancer Res.* **1995**, *55*, 6126–6132.

(38) Tjuvajev, J. G.; Finn, R.; Watanabe, K.; Joshi, R.; Oku, T.; Kennedy, J.; Beattie, B.; Koutcher, J.; Larson, S.; Blasberg, R. G. Noninvasive imaging of herpes virus thymidine kinase gene transfer and expression: a potential method for monitoring clinical gene therapy. *Cancer Res.* **1996**, *56*, 4087–4095.

(39) Morin, K. W.; Duan, W.; Xu, L.; Zhou, A.; Moharram, S.; Knaus, E. E.; McEwan, A. J.; Wiebe, L. I. Cytotoxicity and cellular uptake of pyrimidine nucleosides for imaging herpes simplex type-1 thymidine kinase (HSV-1 TK) expression in mammalian cells. *Nucl. Med. Biol.* **2004**, *31*, 623–630.

(40) Morin, K. W.; Atrazheva, E. D.; Knaus, E. E.; Wiebe, L. I. Synthesis and cellular uptake of 2′-substituted analogues of (E)-5-(2-[^{125}I]iodovinyl)-2′-deoxyuridine in tumor cells transduced with the herpes simplex type-1 thymidine kinase gene. Evaluation as probes for monitoring gene therapy. *J. Med. Chem.* **1997**, *40*, 2184–2190.

(41) Goodchild, J.; Porter, R. A.; Raper, R. H.; Sim, I. S.; Upton, R. M.; Viney, J.; Wadsworth, H. J. Structural requirements of olefinic 5-substituted deoxyuridines for antiherpes activity. *J. Med. Chem.* **1983**, *26*, 1252–1257.

(42) Griengl, H.; Wanek, E.; Schwarz, W.; Streicher, W.; Rosenwirth, B.; Clercq, E. D. 2′-Fluorinated arabinonucleosides of 5-(2-haloalkyl)uracil: synthesis and antiviral activity. *J. Med. Chem.* **1987**, *30*, 1199–1204.

(43) Jin, F.; Xu, Y.-Y. Palladium-catalyzed cross-coupling of (E)-(3-trifluoromethyl-1,3-butadienyl)diisopropoxyborane with vinyl halides. An efficient stereospecific synthesis of trifluoromethylated 1,3,5-trienes. *J. Fluorine Chem.* **1994**, *67*, 1–4.

(44) Matsuhashi, H.; Hatanaka, Y.; Kuroboshi, M.; Hiyama, T. Synthesis of 5-substituted pyrimidine nucleosides through a palladium-catalyzed cross-coupling of alkenylhalosilanes. *Heterocycles* **1996**, *42*, 375–384.

(45) Fulcrand-El Kattan, G.; Goudgaon, N. M.; Ilksoy, N.; Huang, J.-T.; Watanabe, K. A.; Sommadossi, J.-P.; Schinazi, R. F. Synthesis and biological properties of 5-o-carboranyl-1-(2-deoxy-2-fluoro-β-D-arabinofuranosyl)uracil. *J. Med. Chem.* **1994**, *37*, 2583–2588.

(46) Maguire, A. R.; Hladezuk, I.; Ford, A. New methods for the synthesis of N-benzoylated uridine and thymidine derivatives; a convenient method for N-debenzoylation. *Carbohydr. Res.* **2002**, *337*, 369–372.

(47) Greene, T. W.; Wuts, P. G. M. *Protective Groups in Organic Synthesis*, 3rd ed.; Wiley: New York, 1999; p 779.

(48) Choi, S. R.; Zhuang, Z.-P.; Chacko, A.-M.; Acton, P. D.; Tjuvajev-Gelovani, J.; Doubrovin, M.; Chu, D. C. K.; Kung, H. F. SPECT imaging of herpes simplex virus type1 thymidine kinase gene expression by [^{123}I]FIAU. *Acad. Radiol.* **2005**, *12*, 798–805.

JM800501D